SOME DISASSEMBLY REQUIRED

E. Chiang (Berkeley)

DEMOGRAPHICS

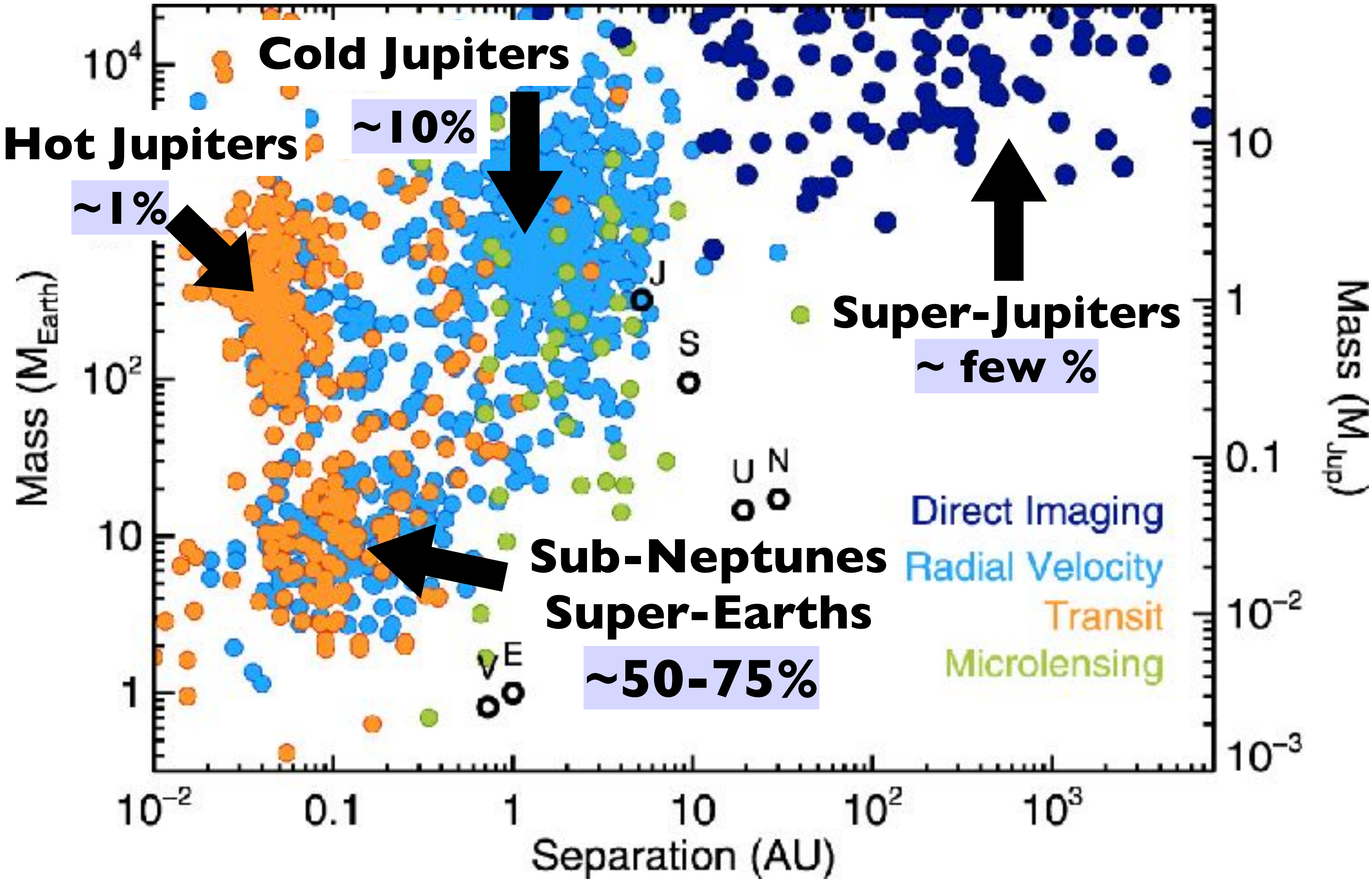

adapted from Bowler 16

1 Myr | 100 Myr | 10 Gyr

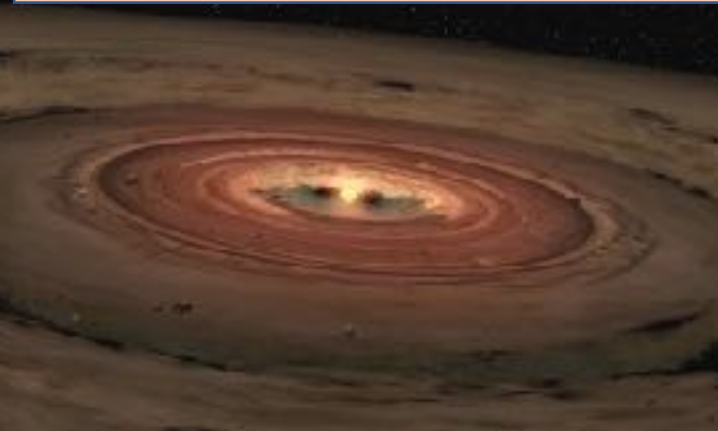

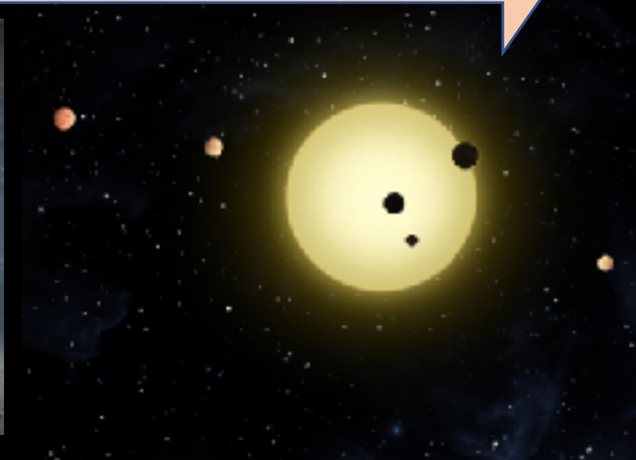

ROCKY PLANET FORMATION

"GIANT IMPACTS ERA"

$$t \sim \frac{M_\oplus}{\Sigma R_\oplus^2} P_{\rm orb} \sim 100\,{\rm Myr}$$

Last (Moon-forming) giant impact @ 50 Myr

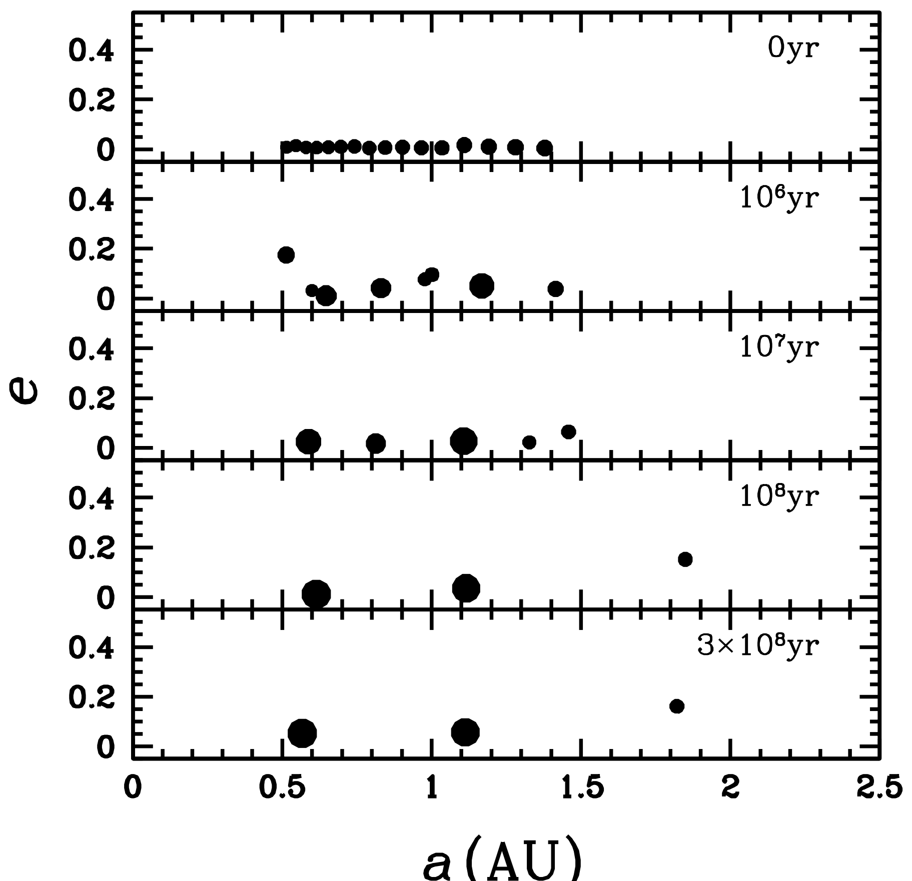

Kokubo & Ida 12

Barboni+17

Faster coagulation $t \sim 1 - 10\,\mathrm{Myr}$

Sub-Neptune gas (1-10% wt.) accreted from gas disc $t_{\mathrm{cool}} \sim t_{\mathrm{gas\,disc}} \sim 1 - 10\,\mathrm{Myr}$

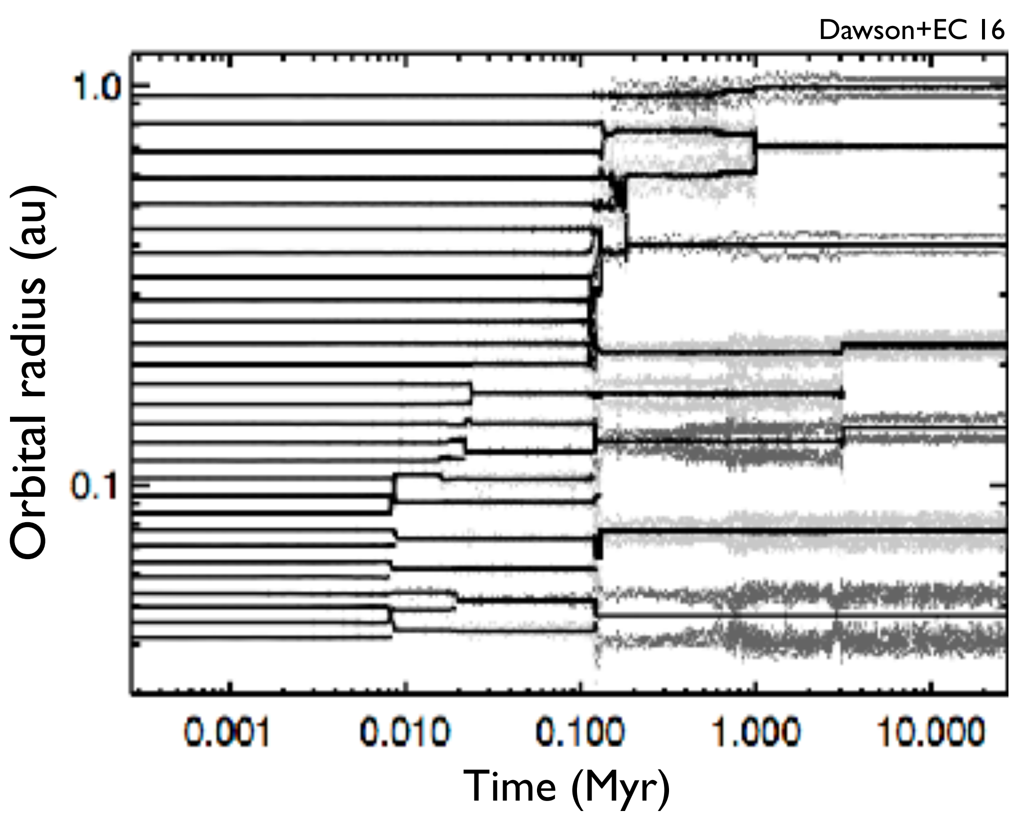

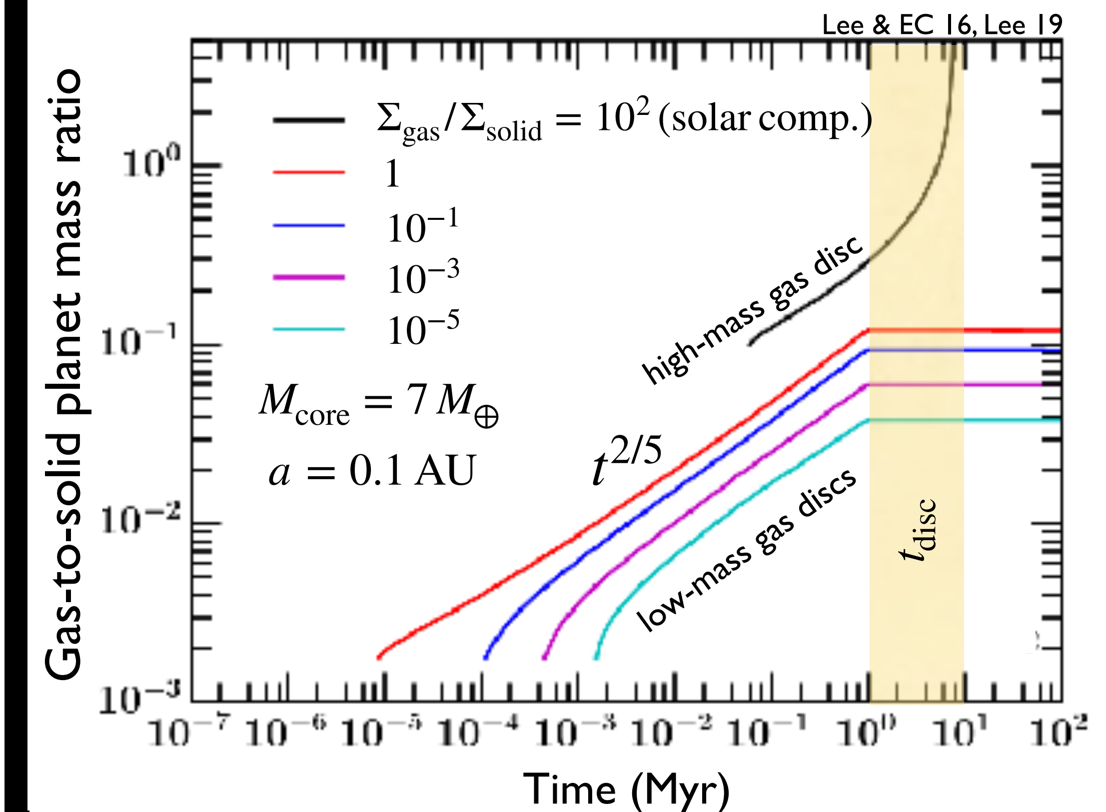

MIGRATION IN GAS DISC

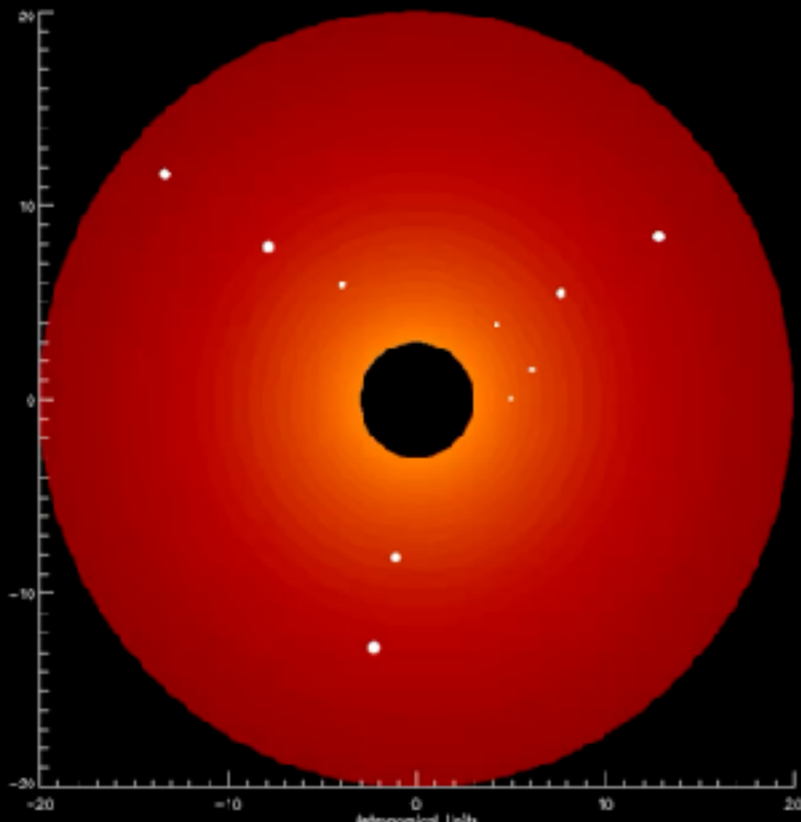

RESONANT CHAIN ASSEMBLY

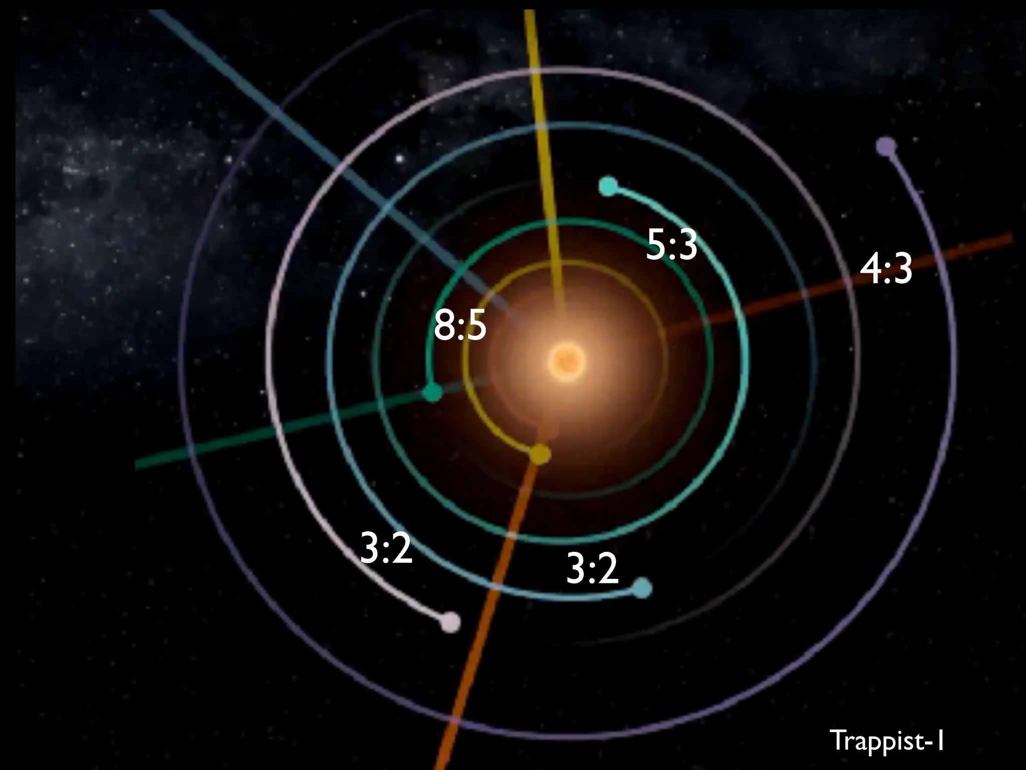

1 - 10 Myr

BREAKING THE CHAINS

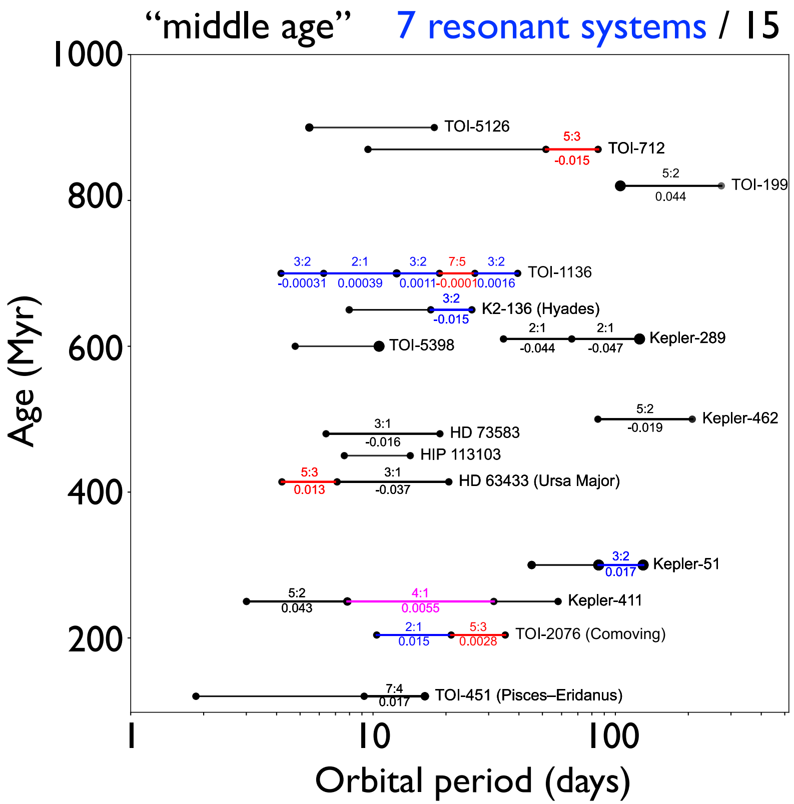

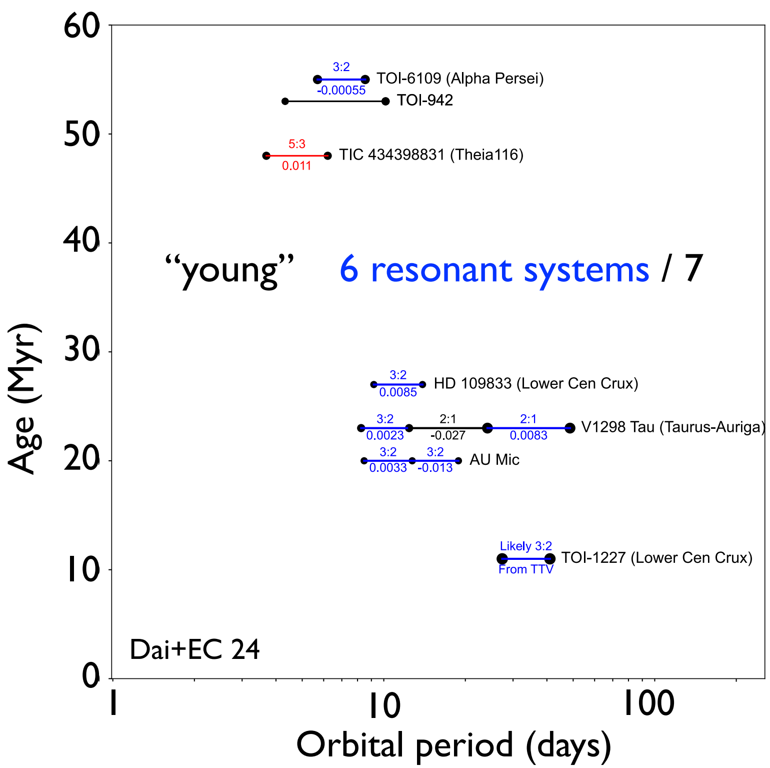

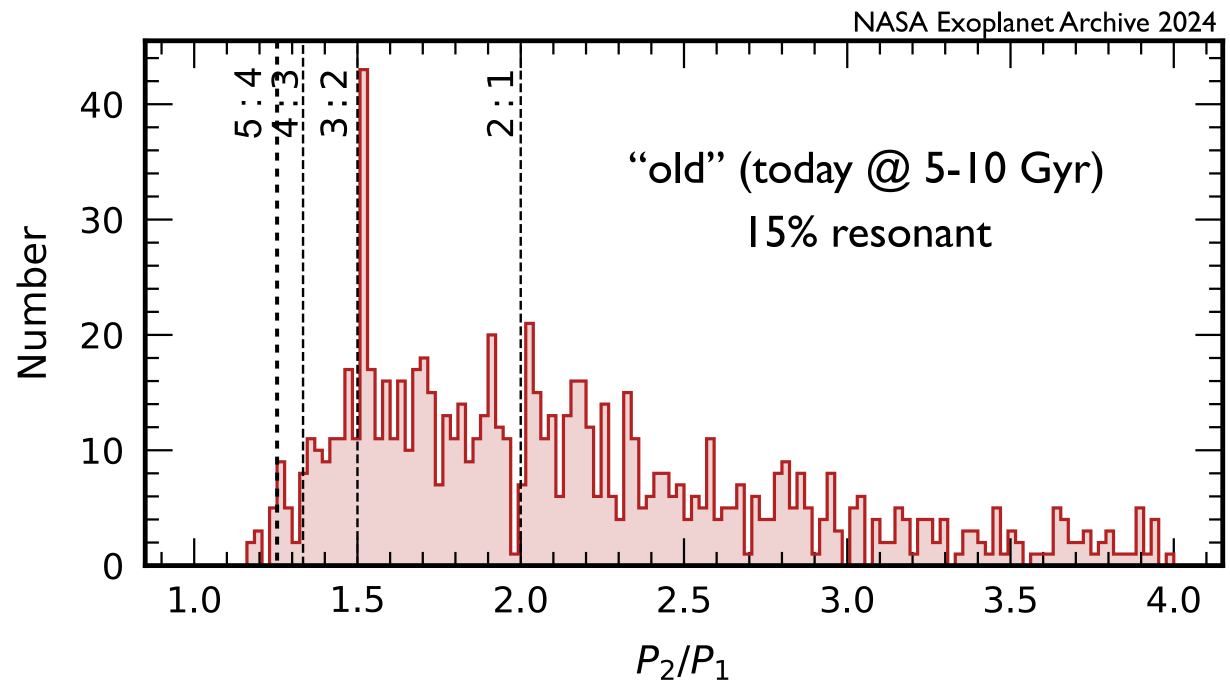

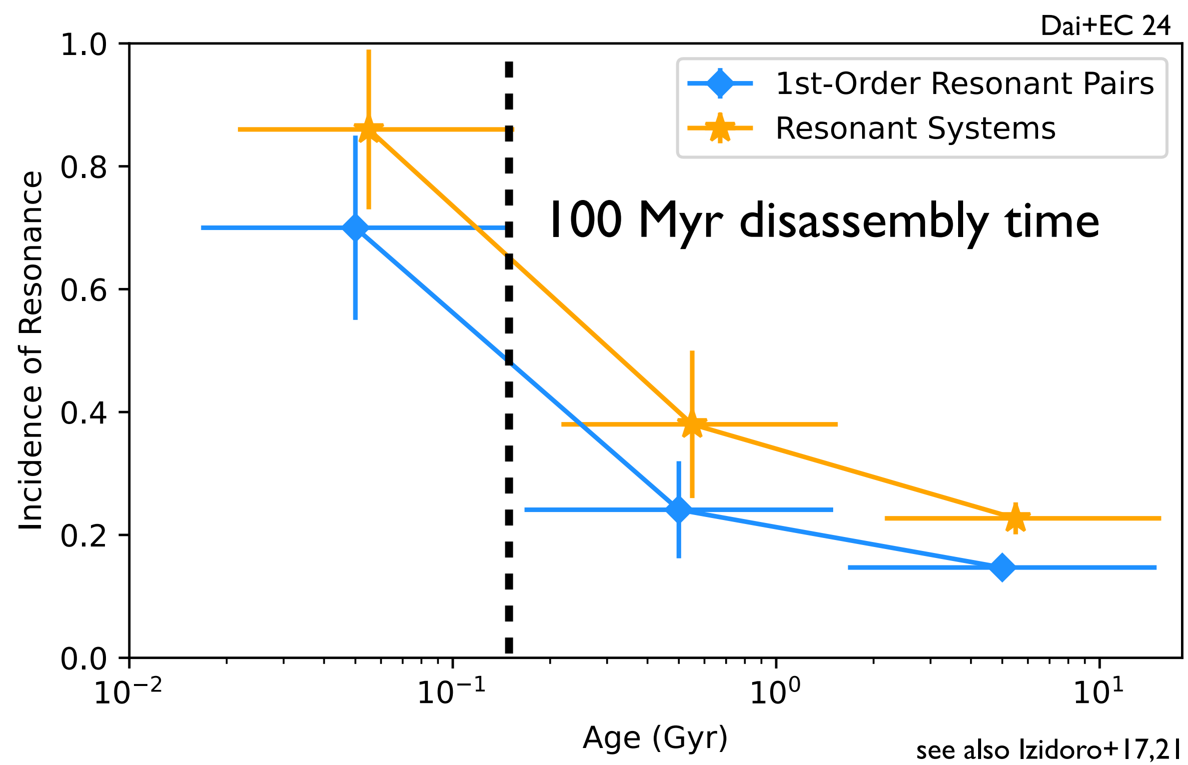

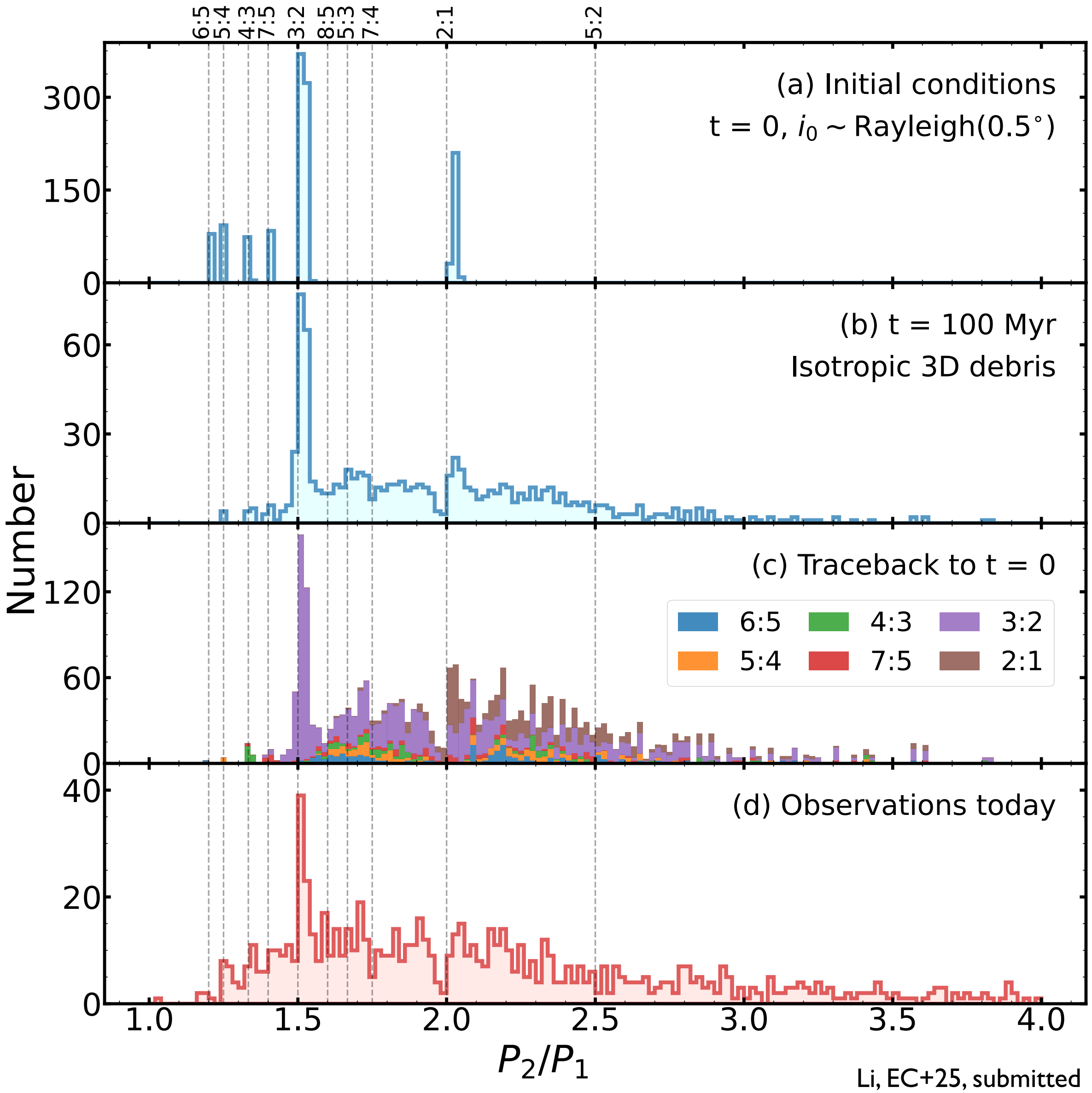

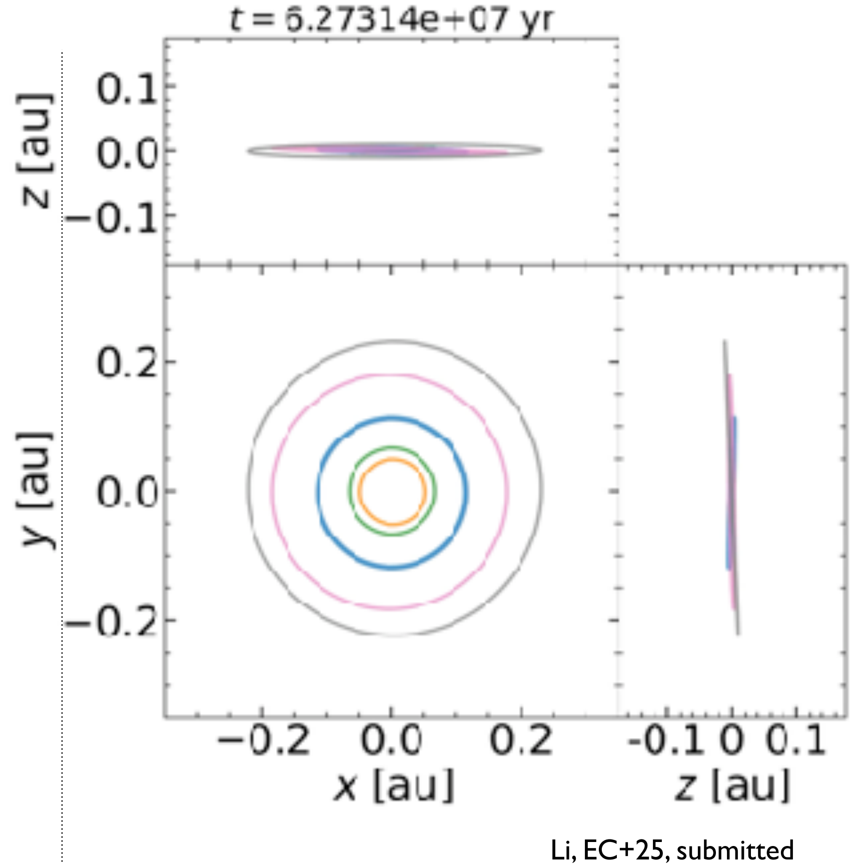

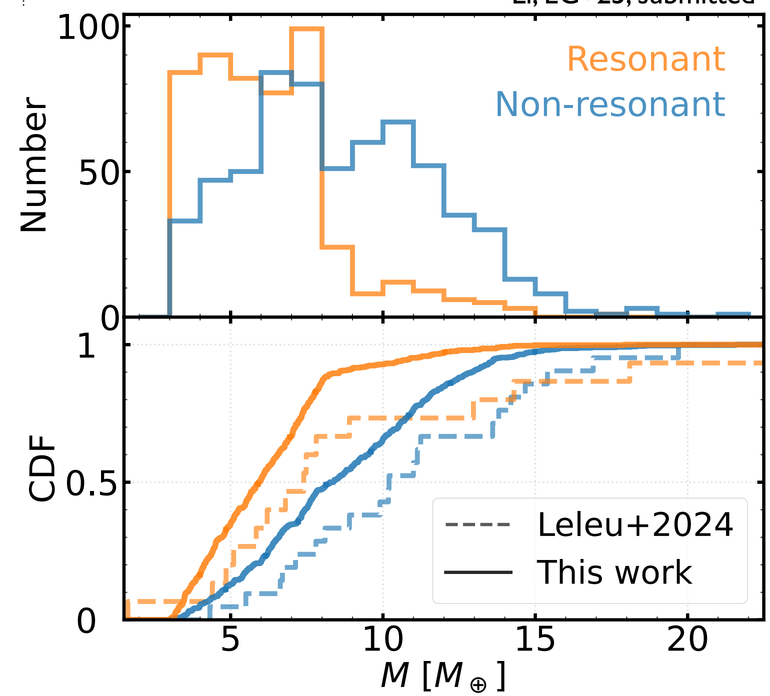

- TTV phases (free eccentricities) > 0 ✔
- Resonant peaks are wide of commensurability ✔
- 2:1 trough is short of commensurability ✔
- Non-resonant (merger) masses > resonant planet masses ✔
- Period ratio continuum ✔
- 100 Myr timescale ?

CATASTROPHIC COLLISIONS IN DEBRIS DISKS

$t \sim 100\,\mathrm{Myr}$

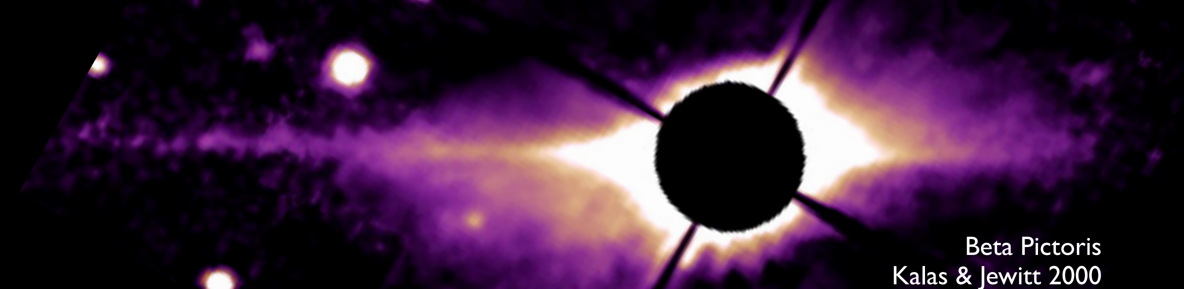

Beta Pictoris
Kalas & Jewitt 2000

HD 172555

Lisse+09, Johnson+12, Schneiderman+21

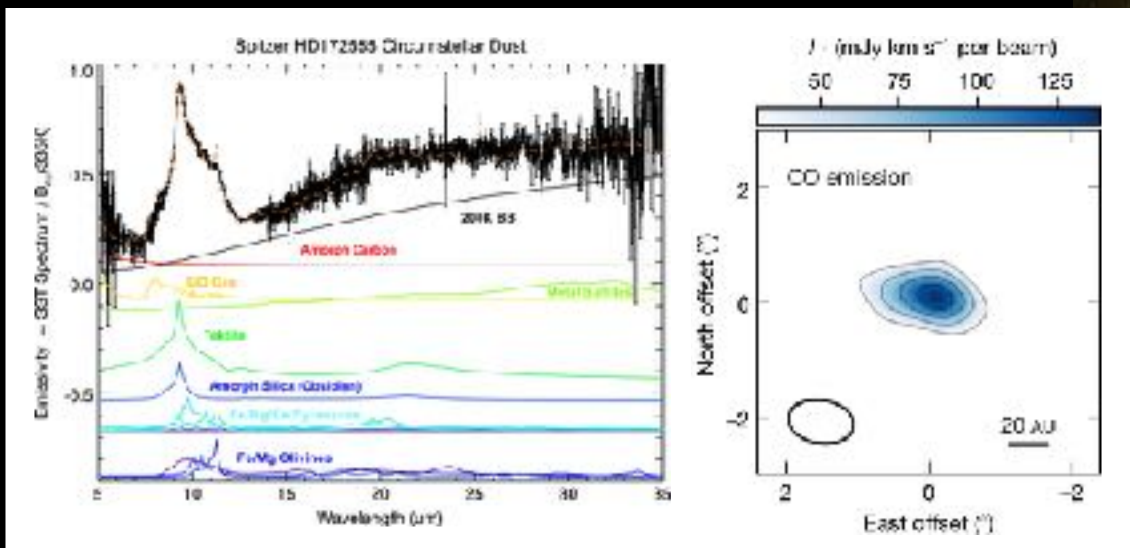

ID 8

Meng+14, 15, Su+19

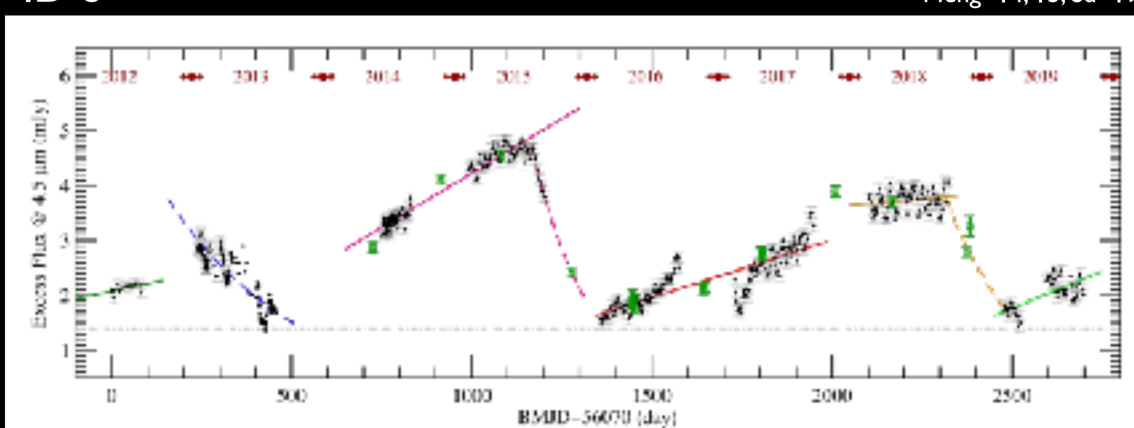

Chen, Su+20, Genda+15

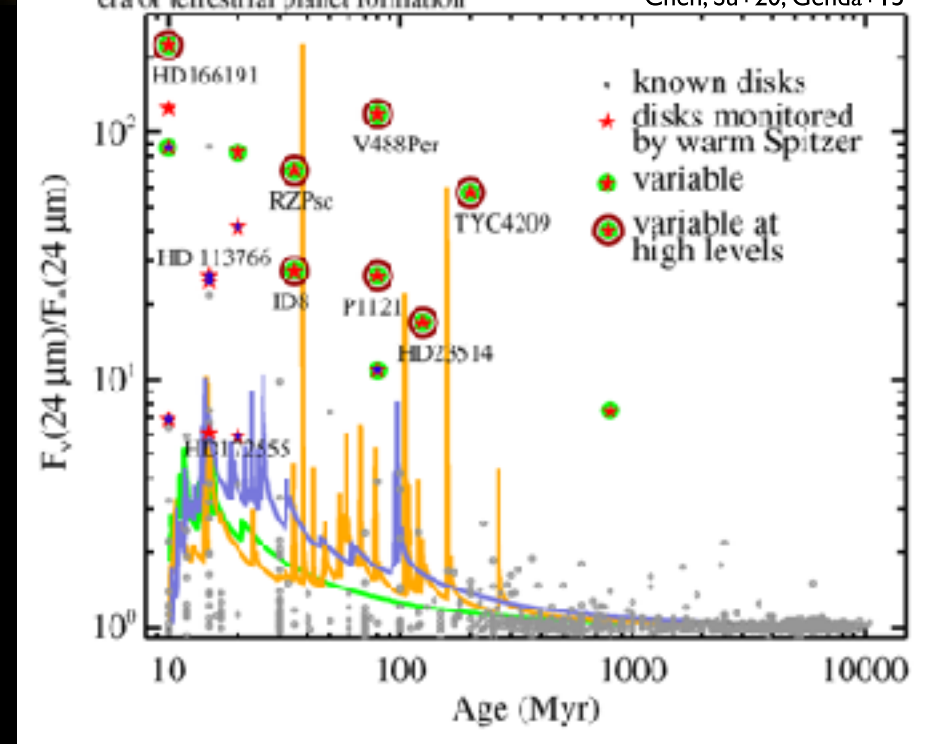

MYSTERIOUS MORPHOLOGIES

WINGED DISKS

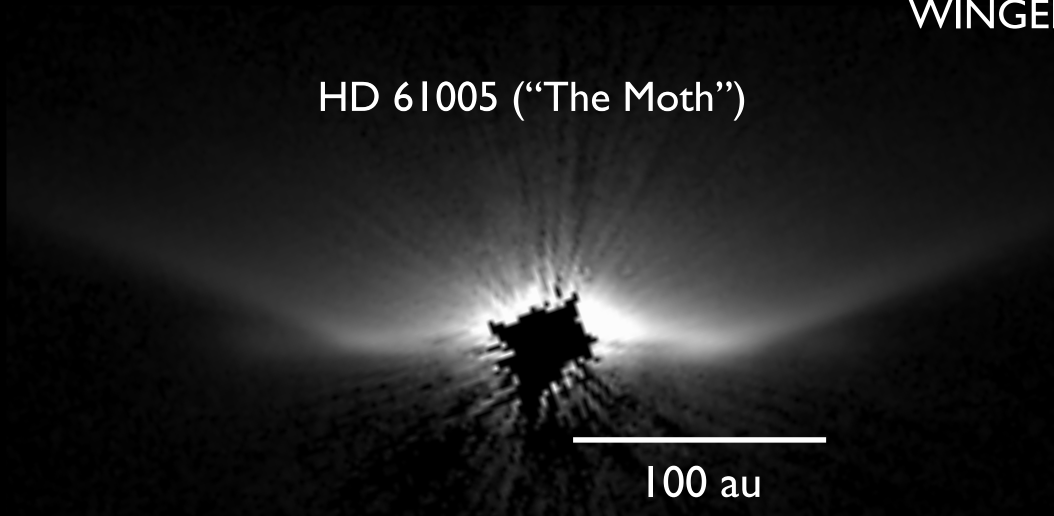

LOPSIDED DISKS

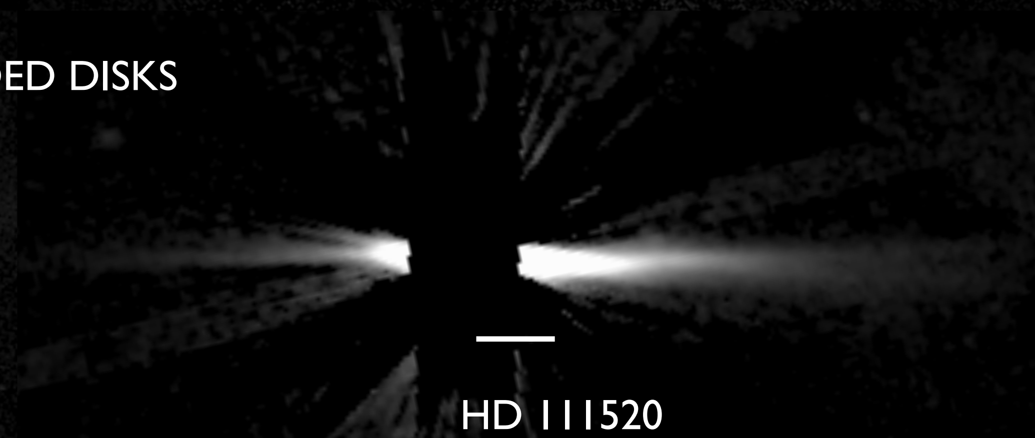

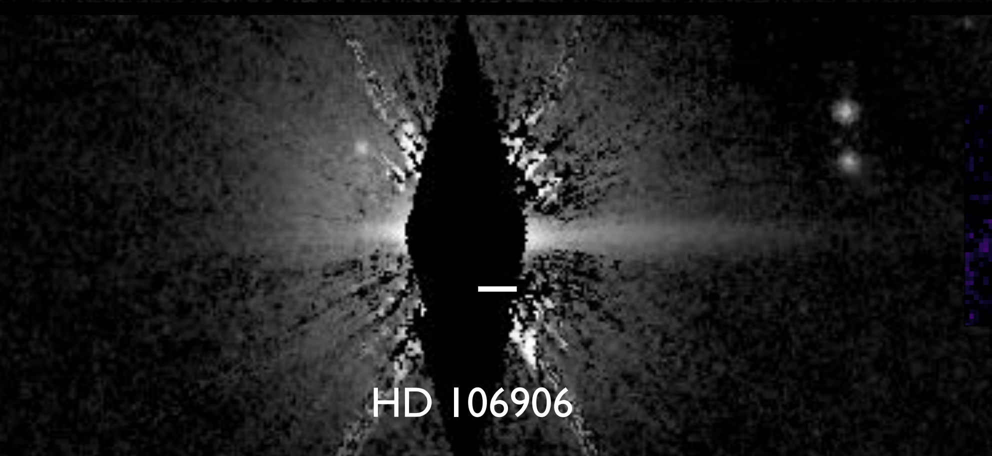

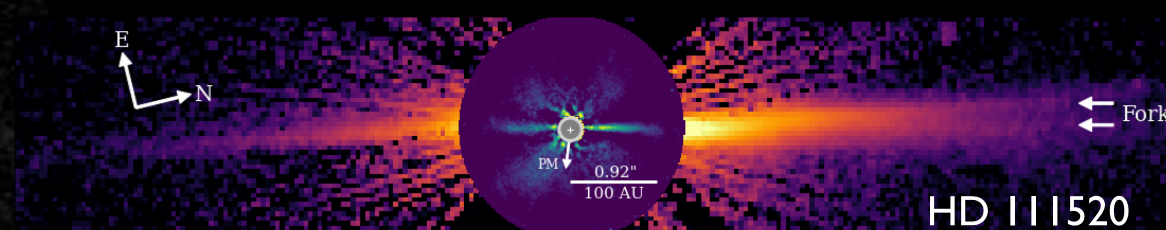

Schneider+14, Padgett & Stapelfeldt 15, Crotts+22

ANATOMY OF A GIANT IMPACT

face-on

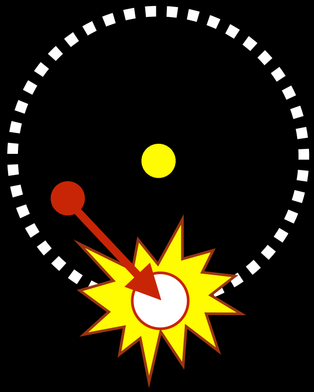

progenitor

edge-on

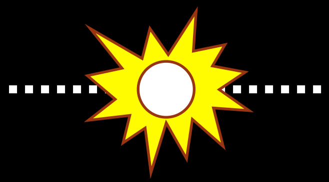

ANATOMY OF A GIANT IMPACT

face-on

$\Delta v_{\mathrm{ejecta}}/v_{\mathrm{orbital}} \sim 0.03$

edge-on

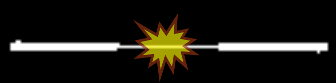

"collision point singularity"

Collision fragments return to original collision point for continued grinding

Jackson+14
Kral+15

ANATOMY OF A GIANT IMPACT

dust blown out by radiation+wind pressure

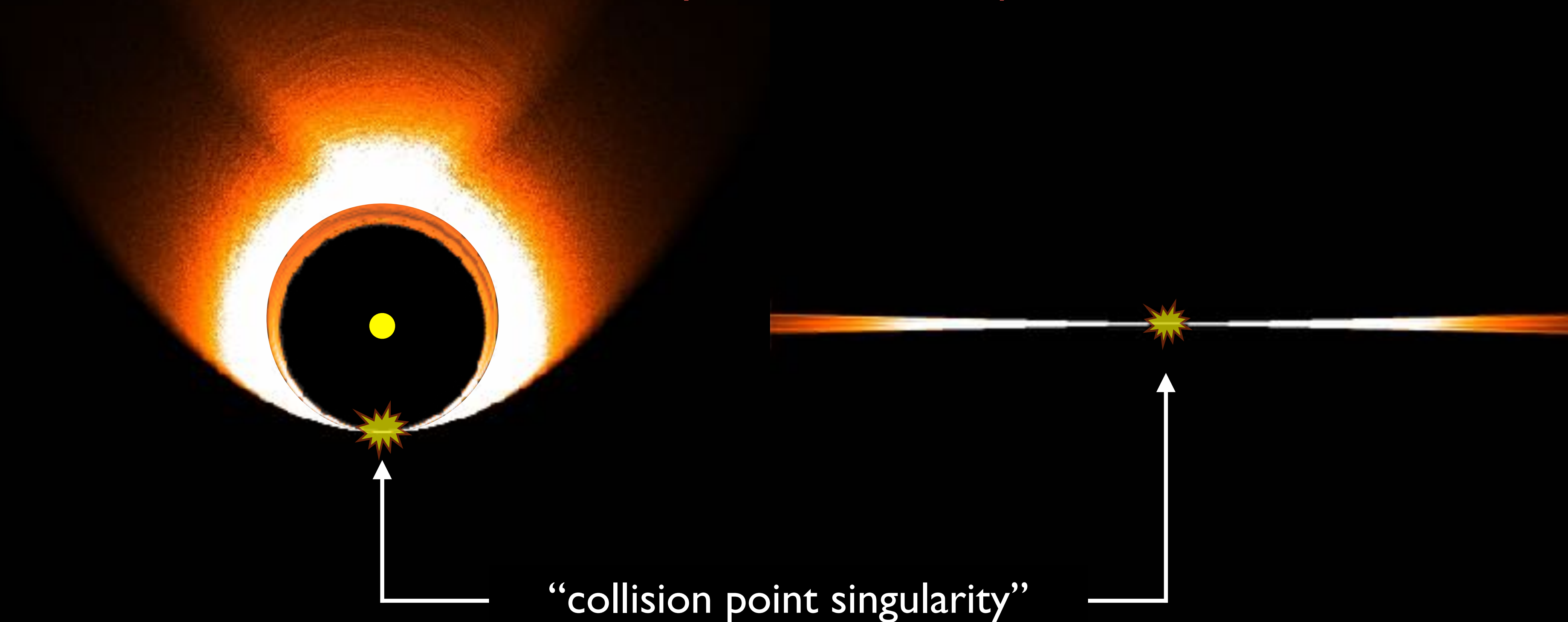

Lee & EC 16
Lin & EC 19
Jones, EC+ 23

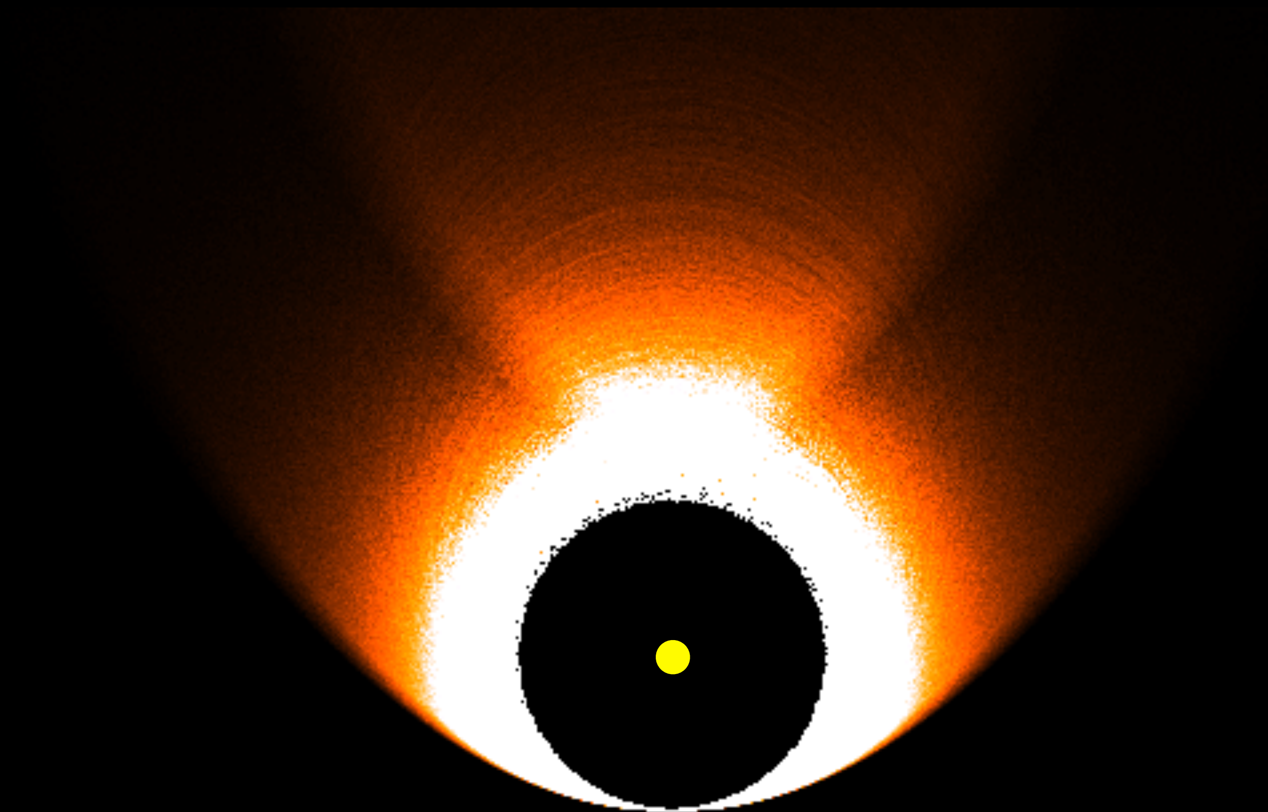

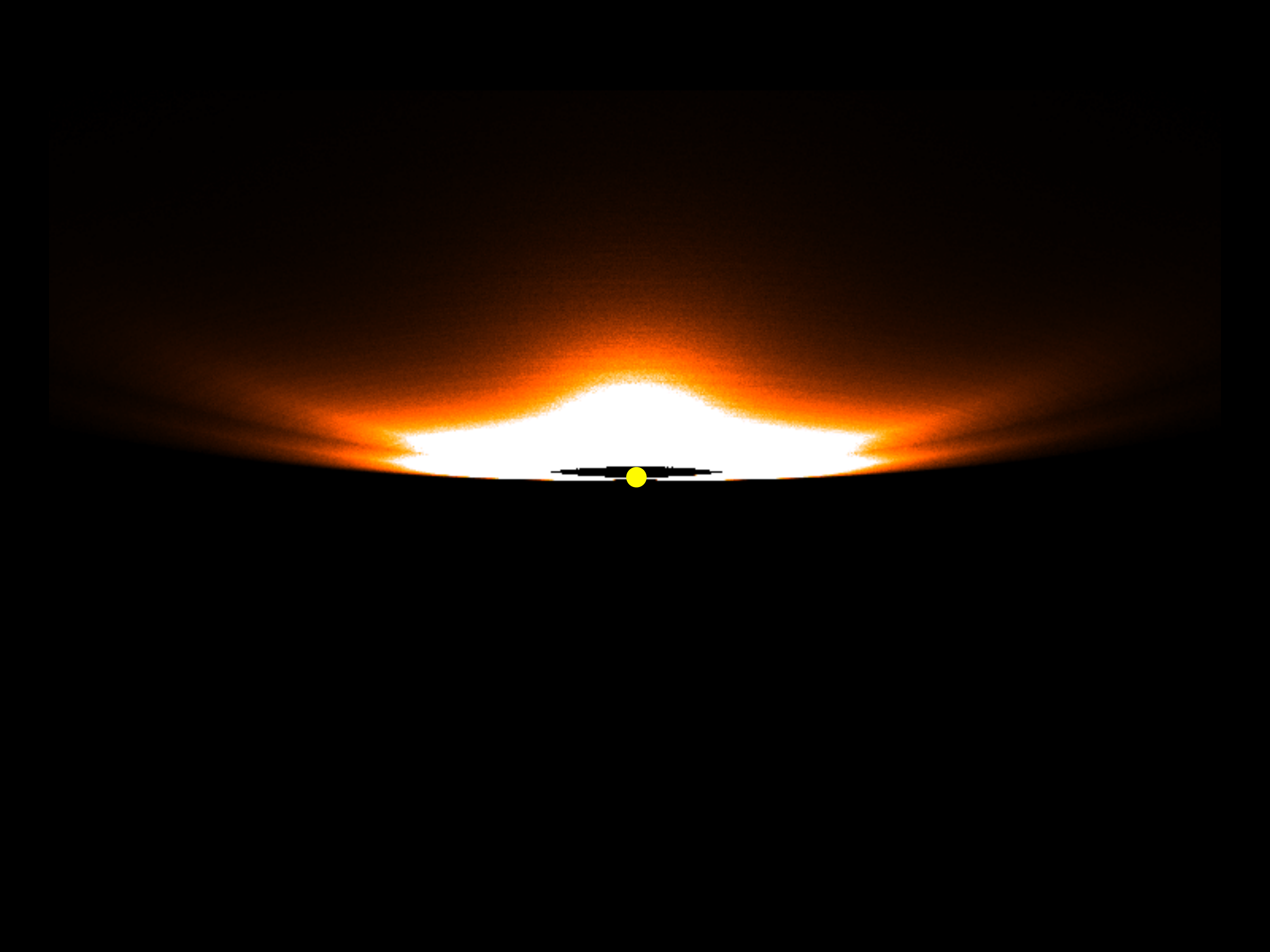

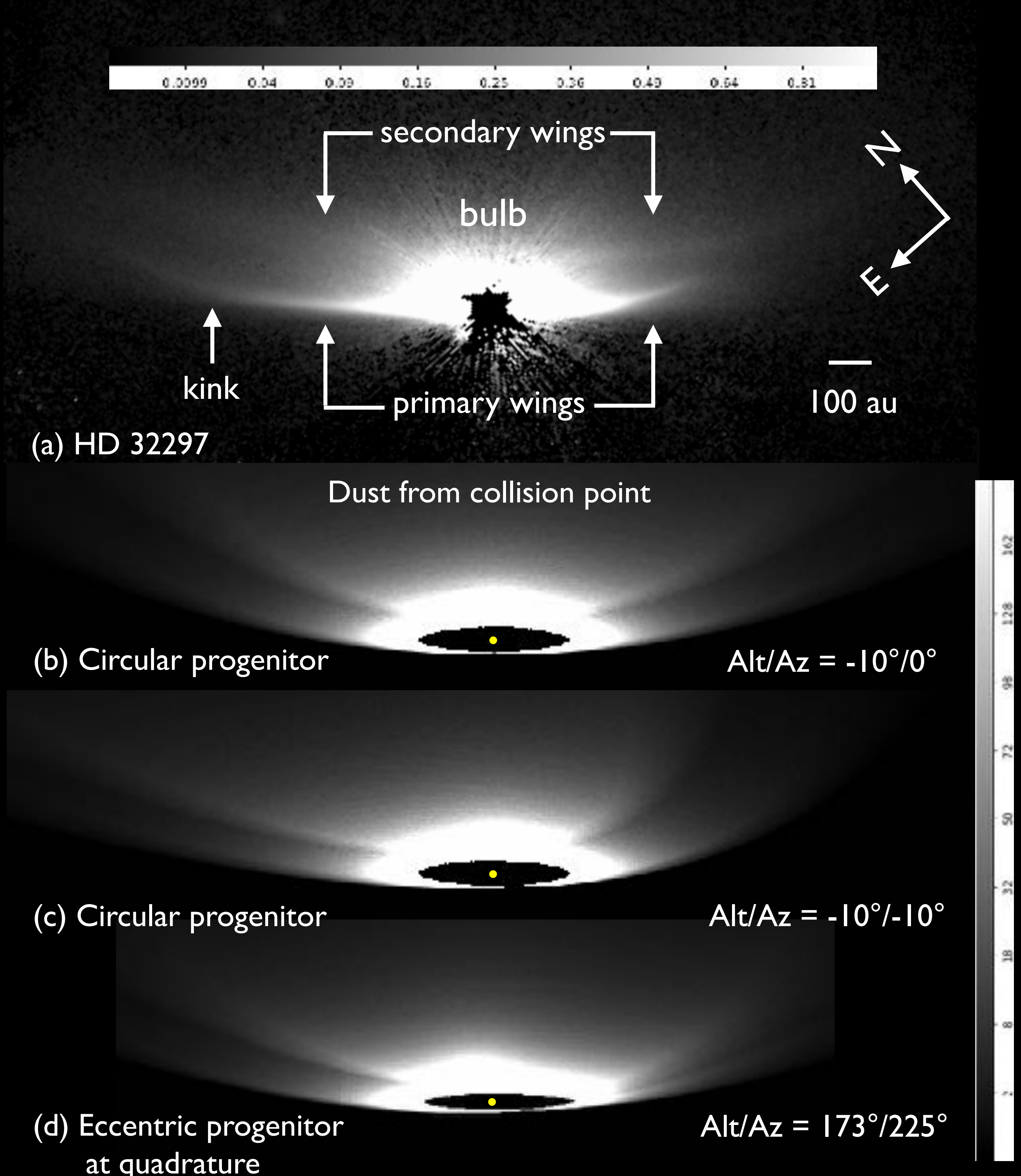
0.0099
0.04
0.09
0.16
0.25
0.36
0.49
0.64
0.81
secondary wings
bulb
N
E
kink
primary wings
100 au
(a) HD 32297
Dust from collision point
(b) Circular progenitor
Alt/Az = -10°/0°
(c) Circular progenitor
Alt/Az = -10°/-10°
(d) Eccentric progenitor
at quadrature
Alt/Az = 173°/225°

Jones, EC+ 23

PROGENITOR MASS

For catastrophic disruption:

$v_{\rm ejecta} > v_{\rm esc,surface}$

$v_{\rm ejecta} \lesssim v_{\rm collision} \sim 1\,{\rm km/s}$

$\Rightarrow$

$R \lesssim 1000\,{\rm km}$

$M \lesssim 3 \times 10^{-3} M_\oplus$

$\lesssim$ Pluto

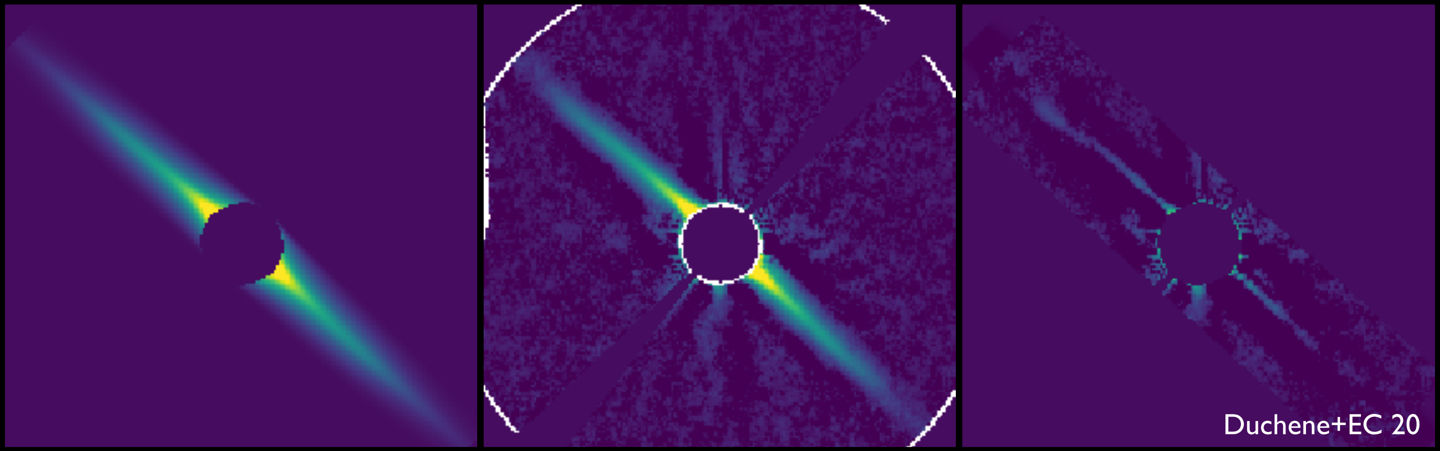

$M_{\rm HD\,32297,H-band} \sim$ Pluto

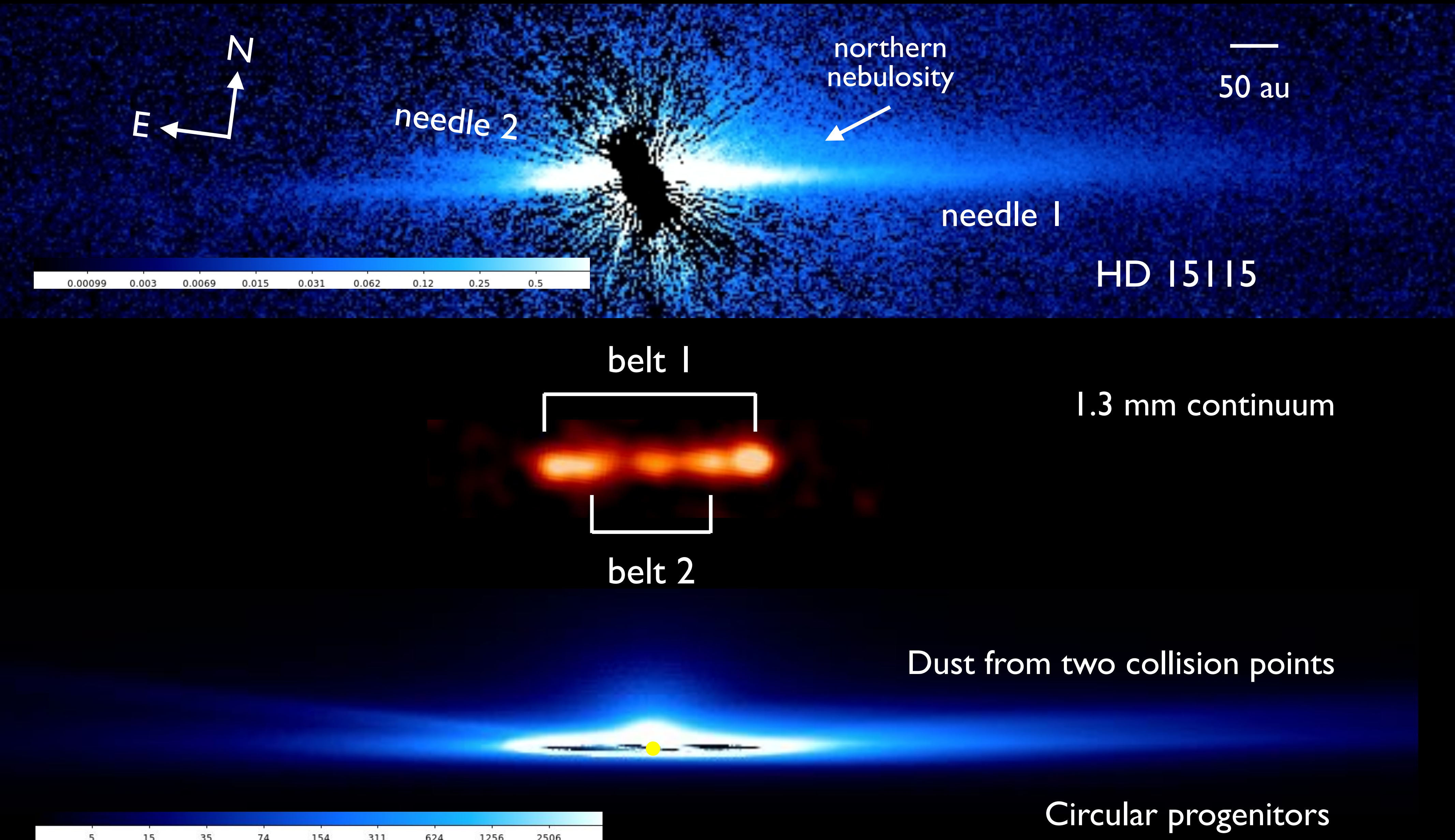
N
E
needle 2
northern nebulosity
50 au
needle 1
HD 15115
0.00099 0.003 0.0069 0.015 0.031 0.062 0.12 0.25 0.5
belt 1
1.3 mm continuum
belt 2
Dust from two collision points
Circular progenitors
5 15 35 74 154 311 624 1256 2506

Jones, EC+ 23

Fast-Moving Features in the AU Mic Disk

Krist+05
Schneider+14

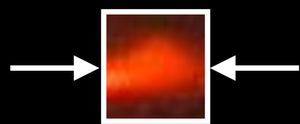

$\Delta\ell_{\rm cloud} \sim 3\,{\rm AU}$

$$B \sim 16\,{\rm mag/arcsec}^2$$

$$M_{\rm cloud} \sim \frac{16\pi\rho_{\rm p} B \Delta\ell^2 a^2 s}{3QPL_*}$$

$$\sim 4\times 10^{-7} M_\oplus \left(\frac{s}{0.1\,\mu{\rm m}}\right)$$

$$t_{\rm cycle} \sim \frac{10\,{\rm AU}}{5\,{\rm km/s}} \sim 10\,{\rm yr}$$

$$\dot{M} \sim \frac{M_{\rm cloud}}{t_{\rm cycle}} \sim 4\times 10^{-8} M_\oplus/{\rm yr}$$

EC & Fung 17

Boccaletti+15

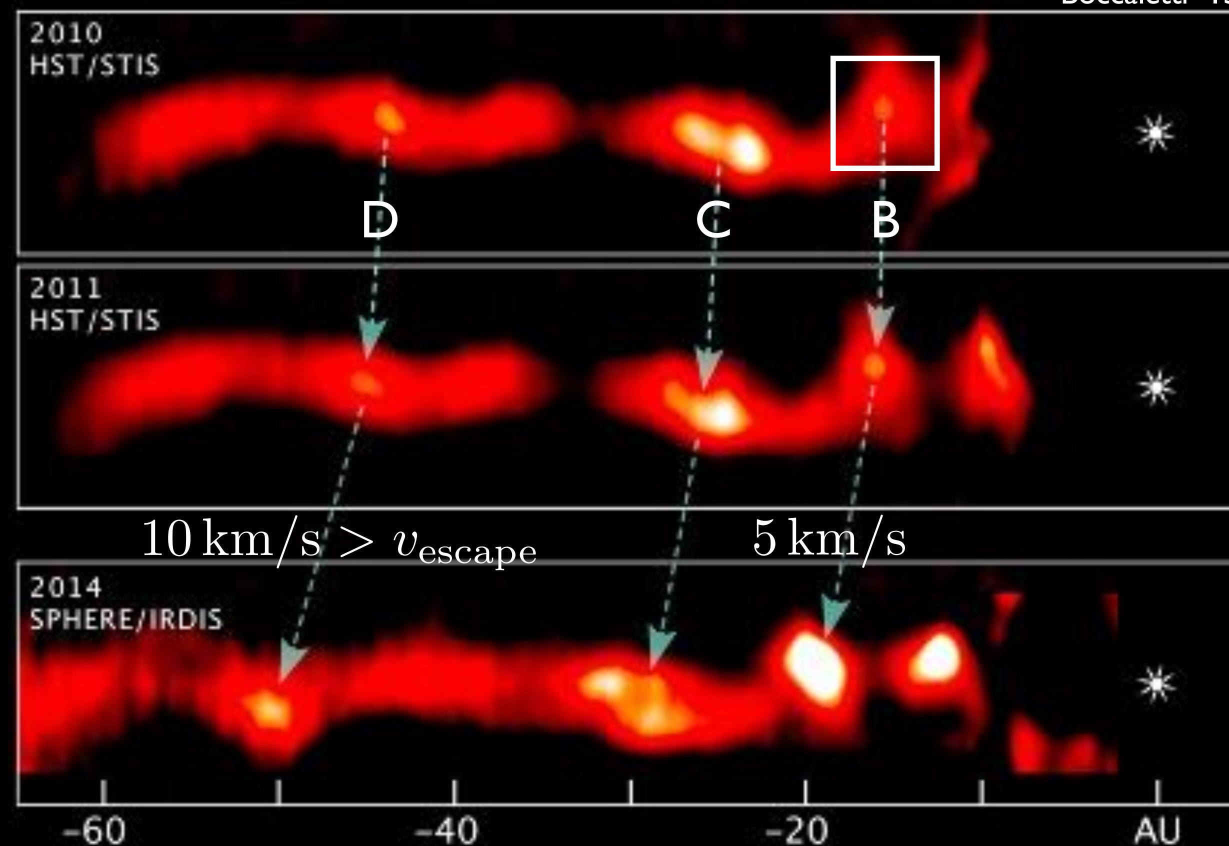

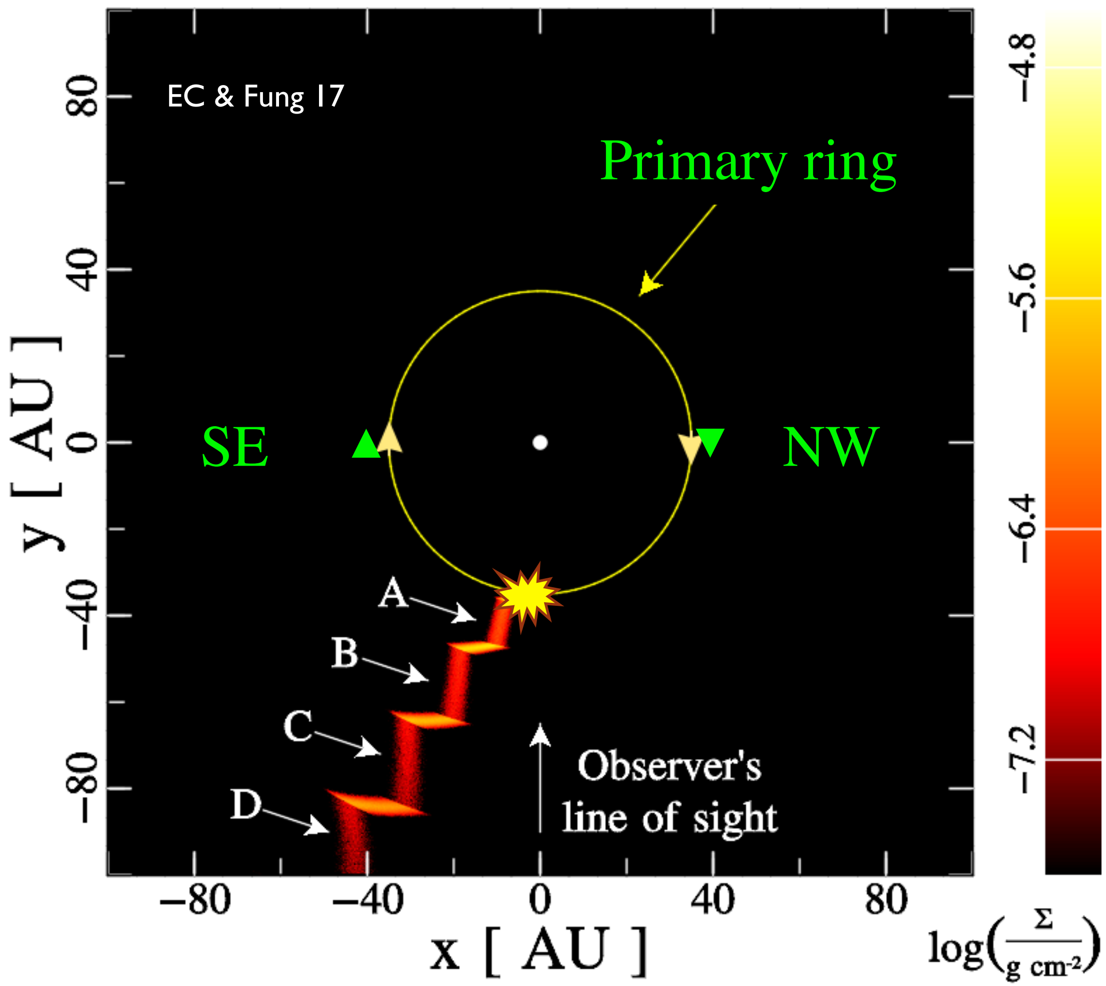

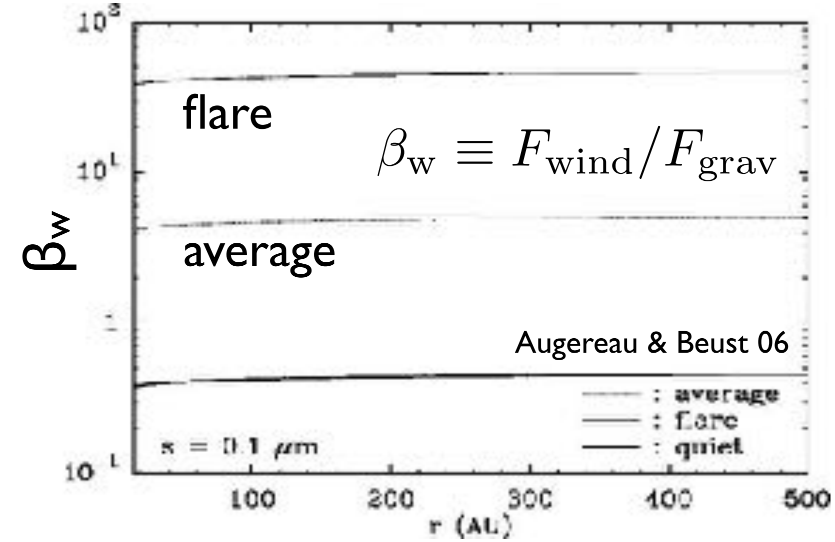

	High	Low
Stellar Mass Loss	$10^3 \dot{M}_\odot$	$10^2 \dot{M}_\odot$
Duration	2.5 yr	7.5 yr
β_w	20	2

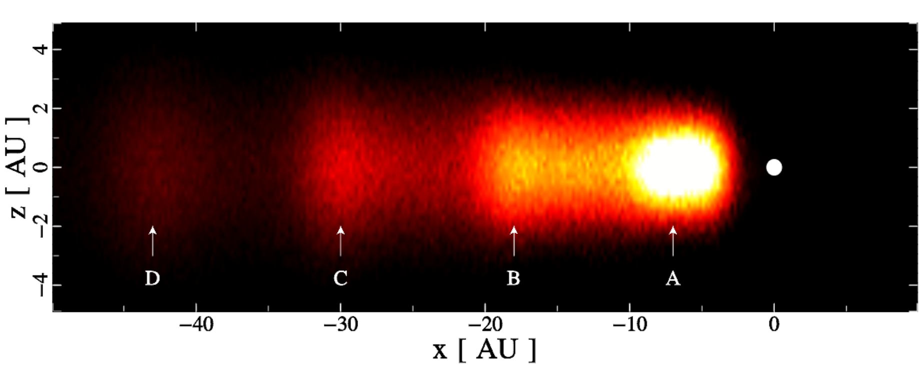

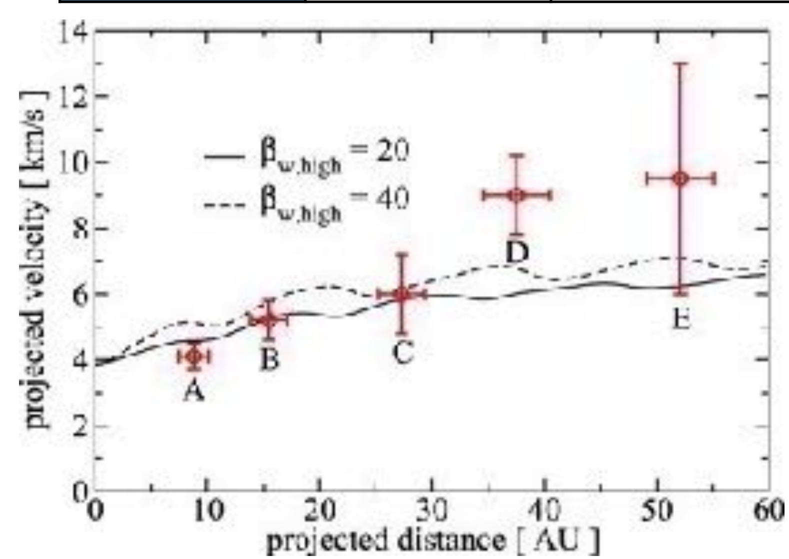

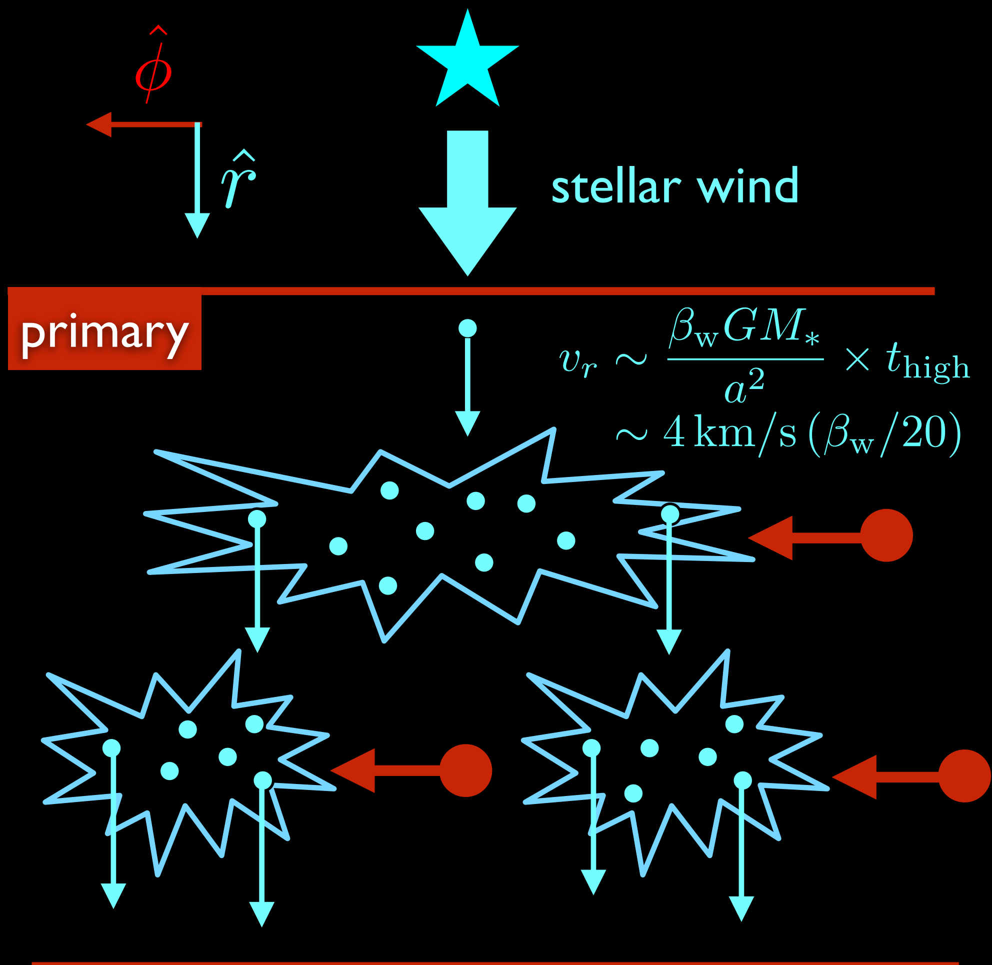

$$v_r \sim \frac{\beta_{\rm w} G M_*}{a^2} \times t_{\rm high}$$
$$\sim 4\,{\rm km/s}\,(\beta_{\rm w}/20)$$

$$\eta \sim \frac{(1/2) m_{\rm bullet} v_r^2}{S^* m_{\rm fragment}} \sim 400$$

$$\dot{M}_{\rm secondary} \times t_{\rm high} \times \exp(\eta \tau_{\rm primary})$$

$$\exp(4) \sim 50$$

$$\sim 4 \times 10^{-7} M_{\oplus}$$ ✔

Artymowicz 97; EC & Fung 17

Giant Impacts and Debris Disk Shapes

Jones, EC+23

Table 1. Possible Explanations for Debris Disk Scattered-Light Asymmetries

Disk ID	Giant Impact	ISM Sculpting	Gravitational Perturber	Comments	References
HD 15115	Y			double needle = double impact	1, 2
AU Mic	Y			collision point avalanches	3
HD 32297	Y	?		double wings	1, 4, 5
HD 61005	?	Y		straight wings + vestigial wings	1, 4, 5, 6
β Pic	Y		Y	needle from giant impact; warp from β Pic b	7, 8, 9, 10
HD 106906	Y		Y	Occam's razor prefers HD 106906b	1, 11, 12, 13
HD 111520			Y	warp analogous to β Pic warp	1, 9

Note—Y = Yes, this seems a viable explanation. ? = Possibly relevant but probably not a dominant effect.

References—1. This paper 2. Mazoyer et al. (2014) 3. Chiang & Fung (2017) 4. Debes et al. (2009) 5. Maness et al. (2009) 6. Olofsson et al. (2016) 7. Dent et al. (2014) 8. Janson et al. (2021) 9. Mouillet et al. (1997) 10. Dupuy et al. (2019) 11. Lee & Chiang (2016) 12. Rodet et al. (2017) 13. Moore et al. (2023)

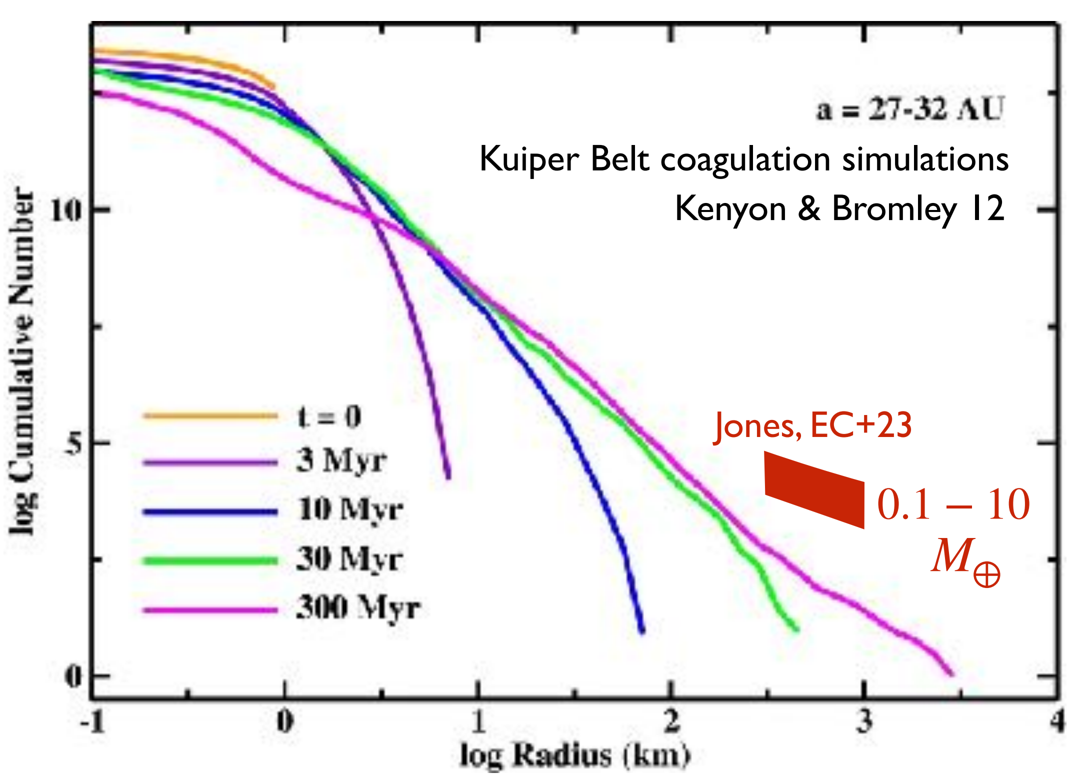

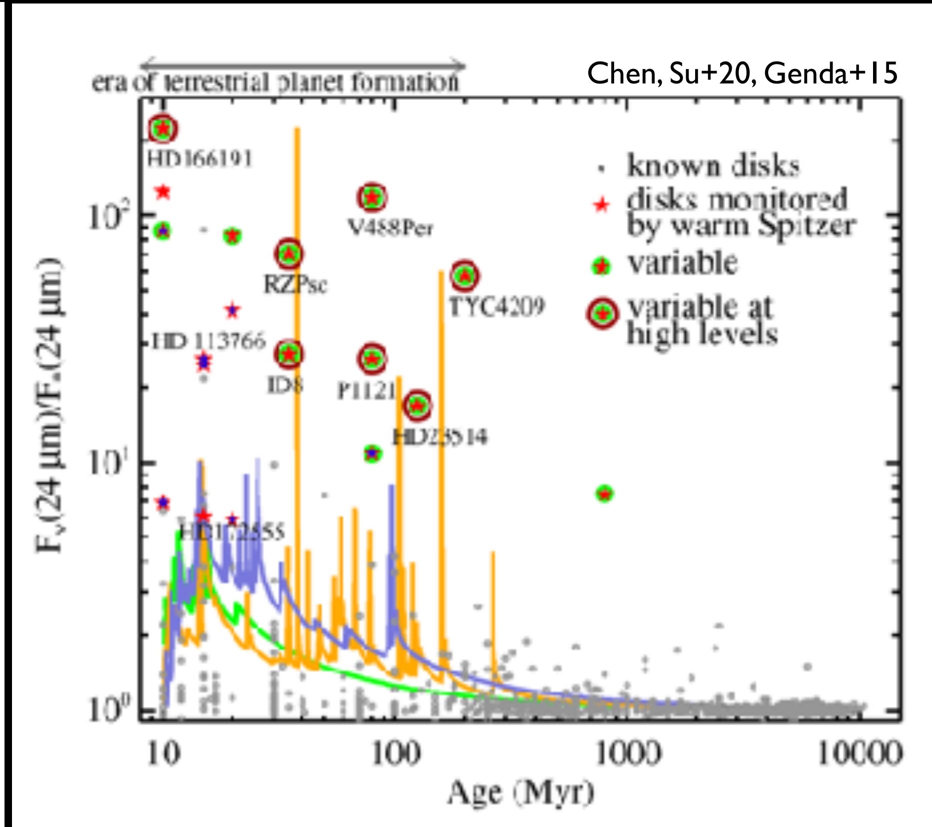

CHONDRULES

- 0.1-1 mm igneous spheres
- 30-99% volume fraction
- near-solar composition
- 4.562-4.567 Gyr old

Connelly+12

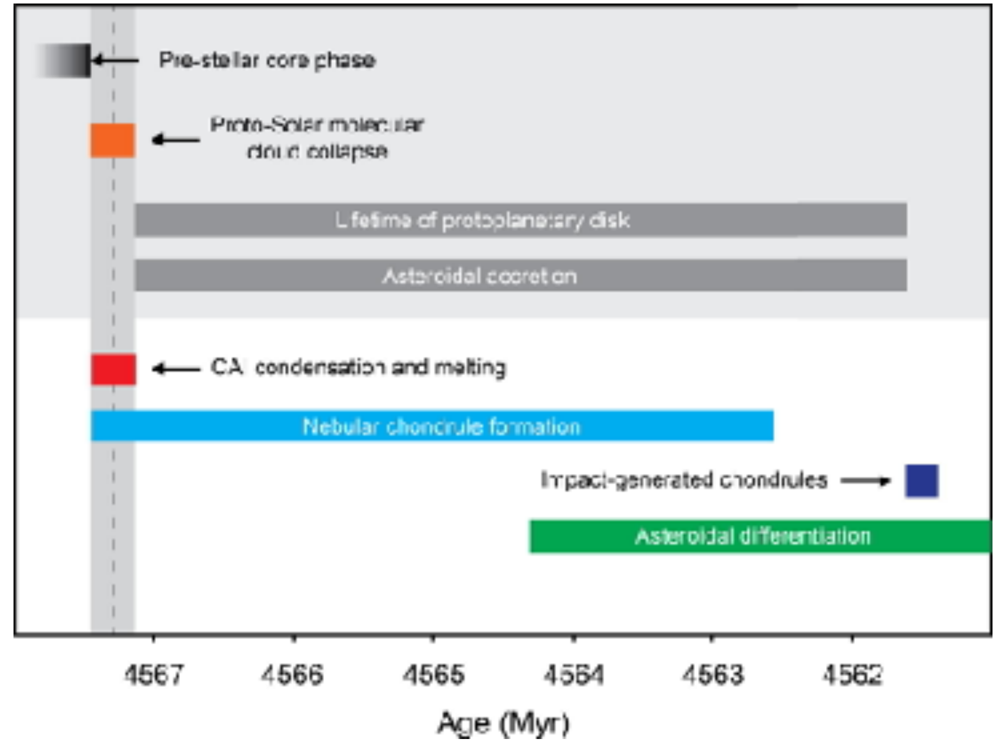

Campbell+02, Krot 05

CB/CH CHONDRITES FROM GIANT IMPACTS

Late-time formation

NATURE|Vol 436|18 August 2005

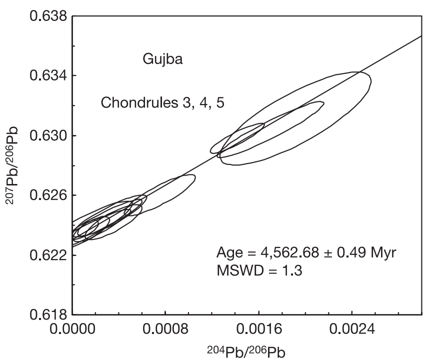

Figure 2 | $^{204}Pb/^{206}Pb$–$^{207}Pb/^{206}Pb$ isochron diagram for three Gujba chondrules (numbers 3, 4 and 5). $^{207}Pb/^{206}Pb$ ratios are not corrected for initial common Pb. Error ellipses are 2σ. Isochron age errors are 95% confidence intervals. MSWD, mean square of weighted deviates.

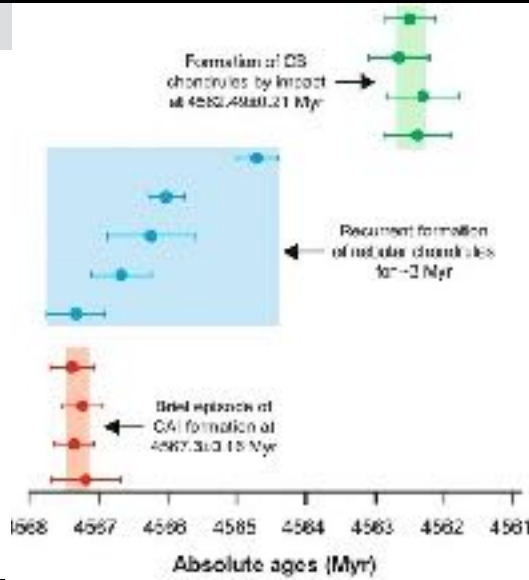

CHRISTIE'S

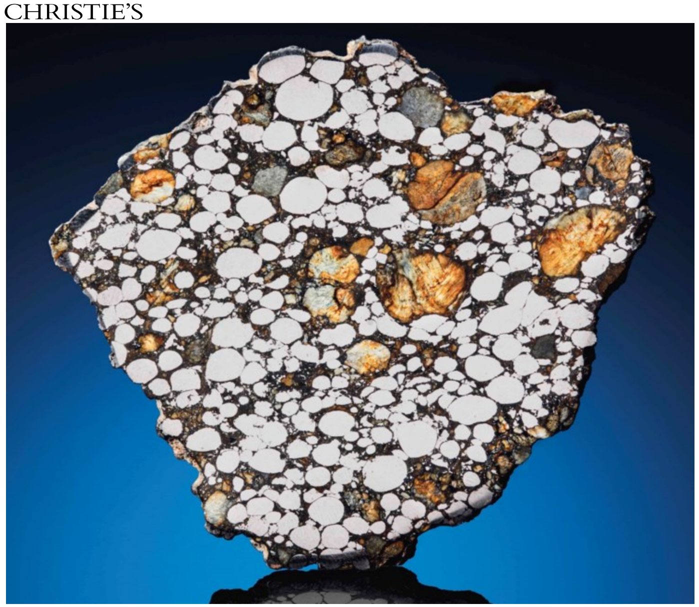

COMPLETE SLICE OF THE SINGULAR GUJBA METEORITE

High-pressure condensation

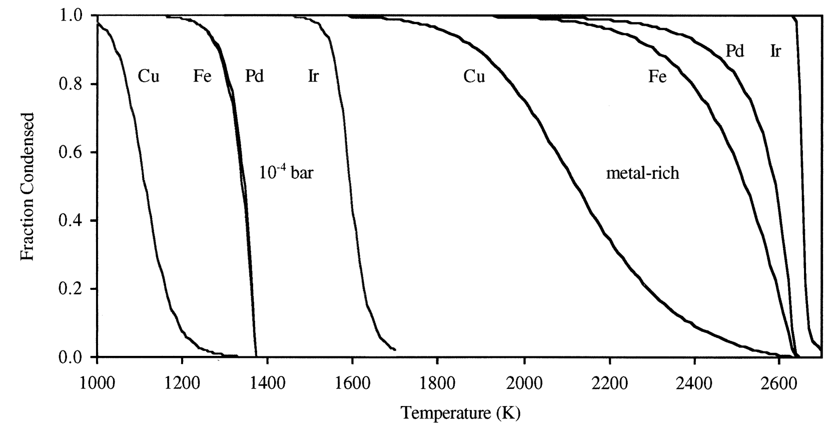

Fig. 6. Condensation curves for Fe, Cu, Pd, and Ir under nebular and metal-rich conditions. Gray curves, at lower temperatures, represent condensation of solid metal alloy from a solar gas at 10^{-4} bar total pressure. Black curves, at higher temperatures, represent condensation of liquid metal alloy from a gas that is uniformly enriched in the siderophile elements by a factor of 10^7 relative to the solar gas. Note that Pd is significantly more refractory than Fe in the metal-rich gas, in contrast to its behavior in solar gas, while Ir is highly refractory relative to Fe in both cases.

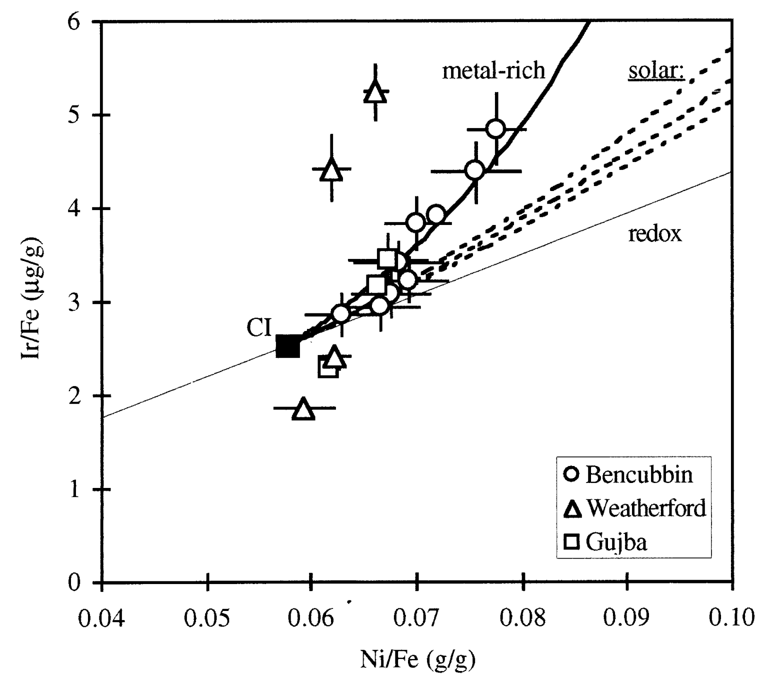

CHONDRULE COOLING CURVES

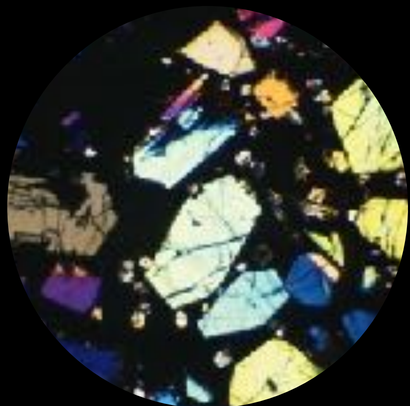

natural

synthetic

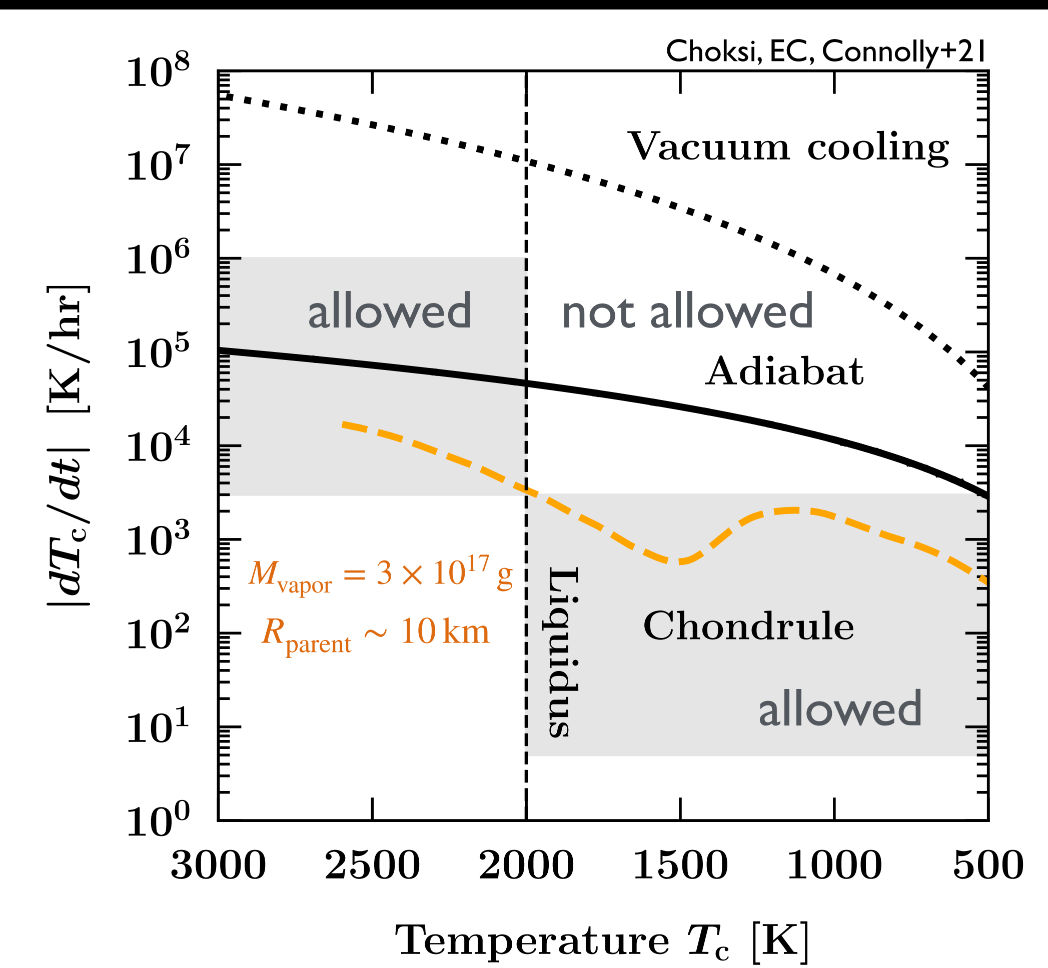

Impact vapor plume expansion

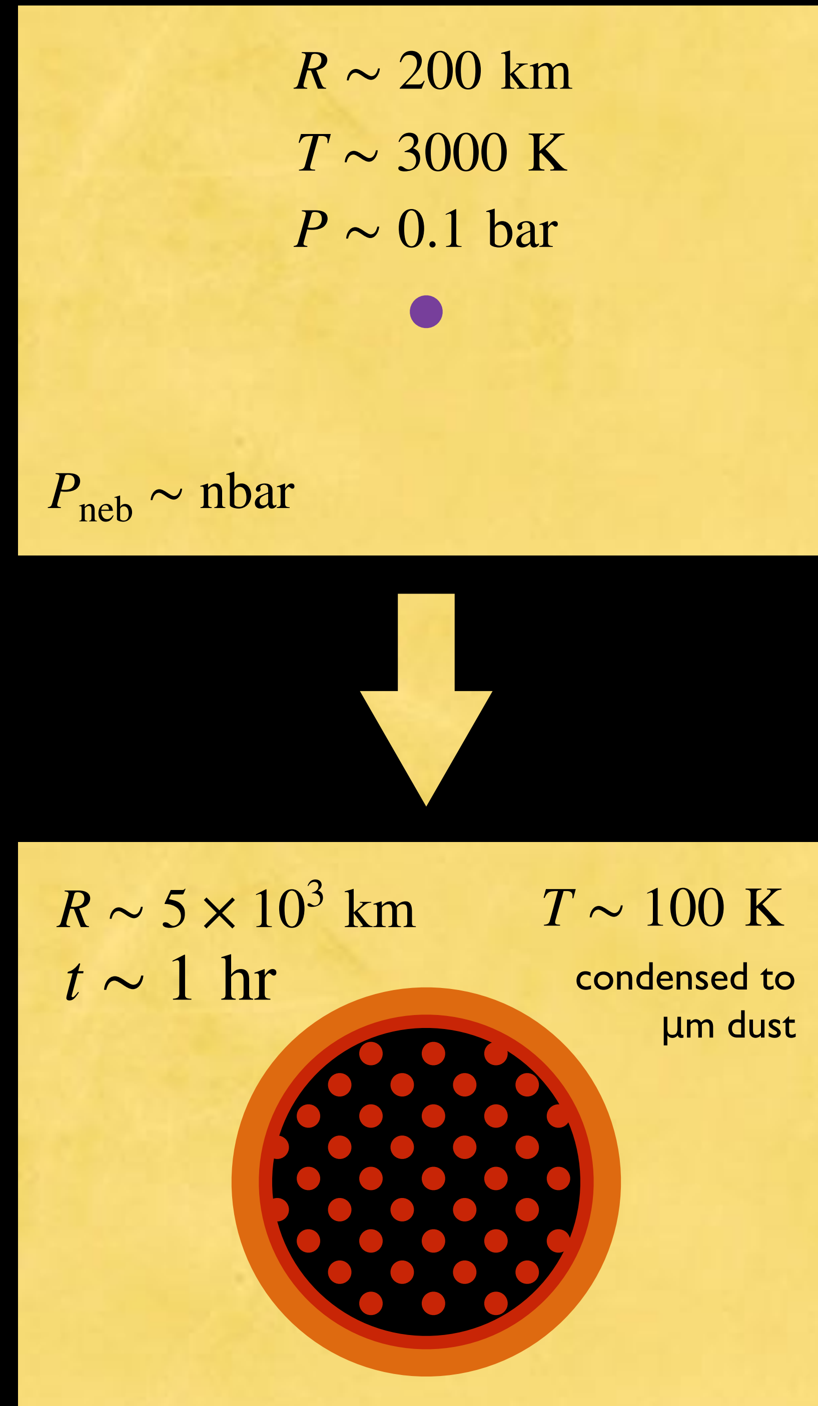

CHONDRULE COOLING CURVES

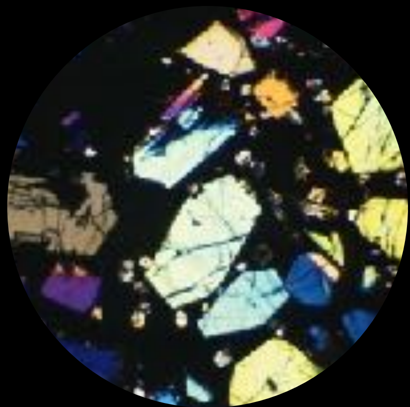

natural

synthetic

For $dT_c/dt \sim -(100 - 1000)\,\mathrm{K/hr}$,

$R_{\mathrm{parent}} \sim 10 - 100\,\mathrm{km}$

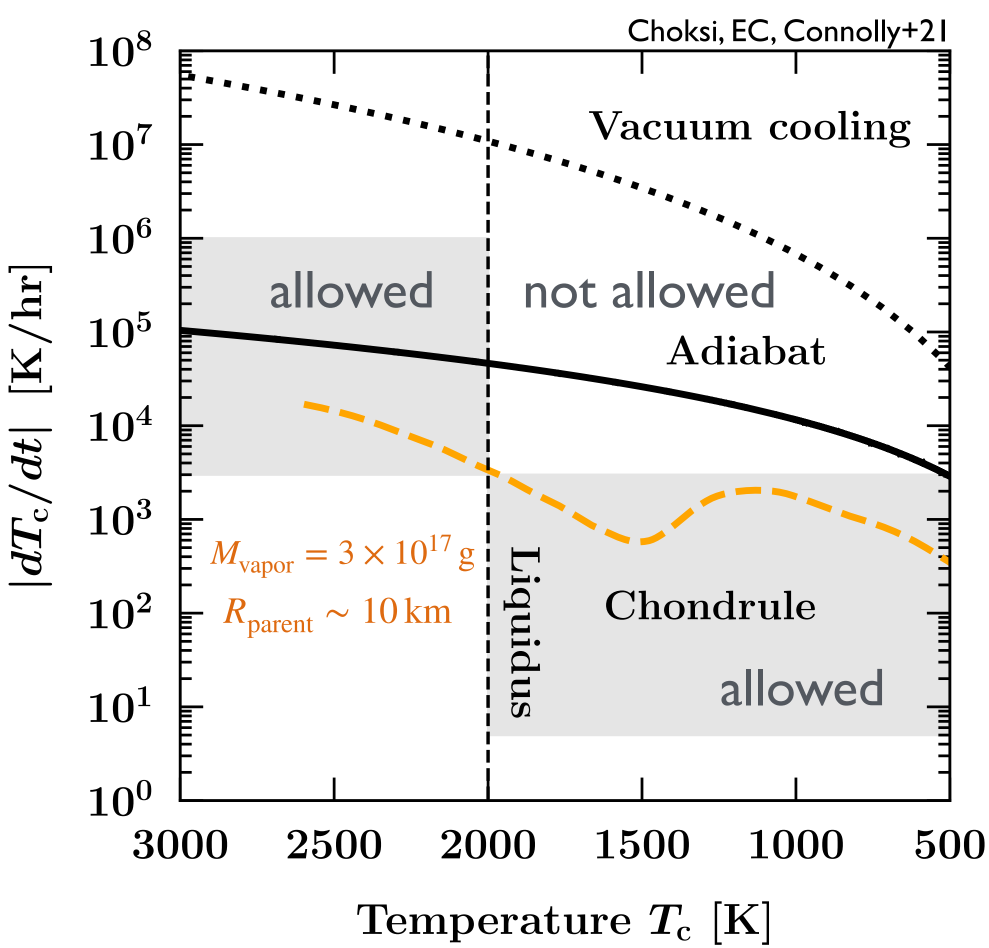

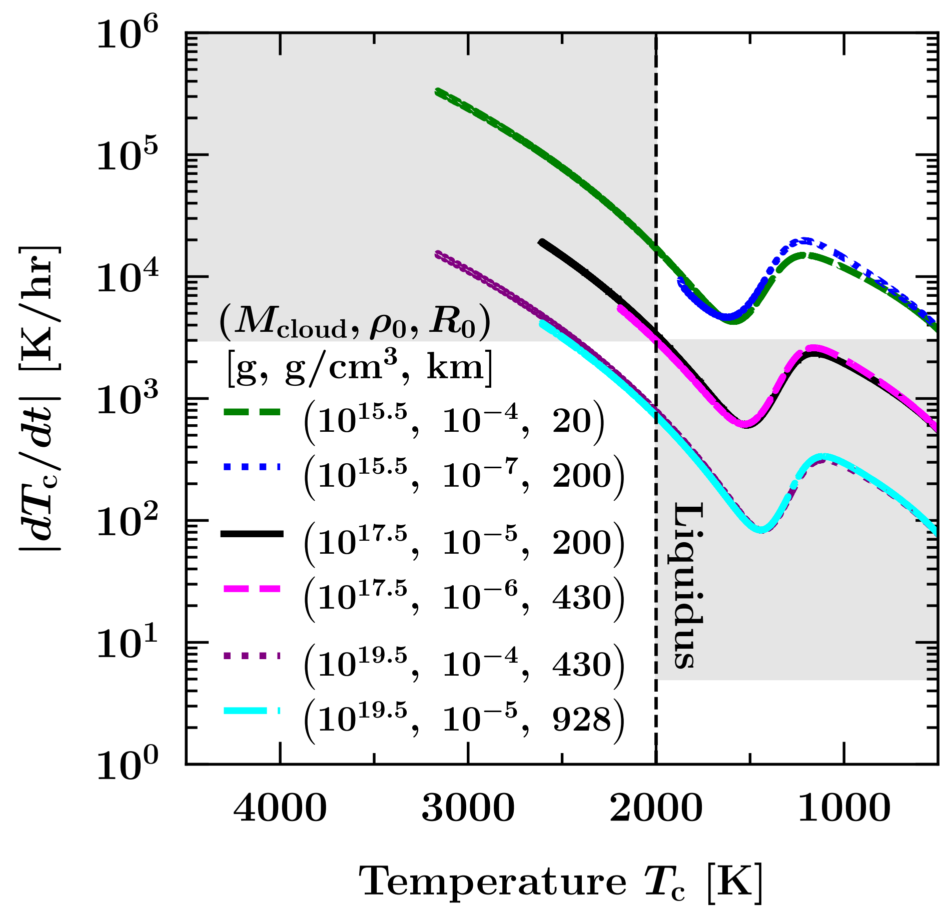

RE-ASSEMBLY BY RADIATION-CONDENSATION INSTABILITY

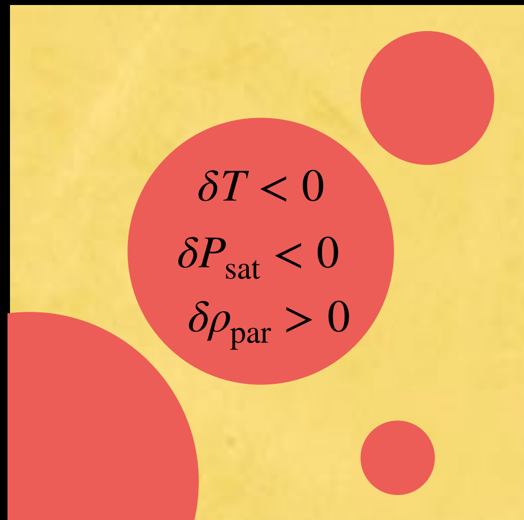

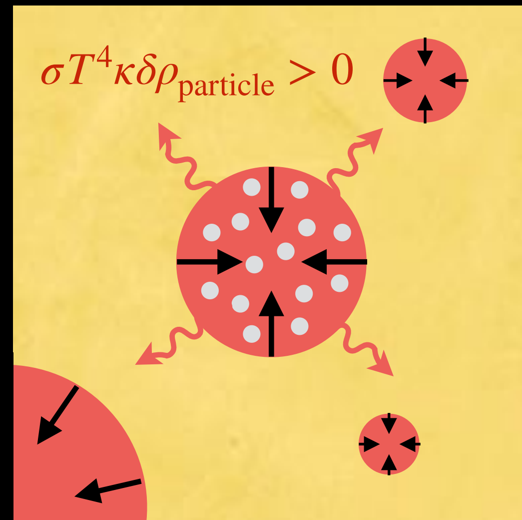

Linear stability analysis

$$\frac{D\rho_{\rm gas}}{Dt} = \frac{d\rho_{\rm sat}}{dT}\frac{DT}{Dt}$$

$$\frac{D\rho_{\rm par}}{Dt} = -\rho_{\rm gas}\nabla\cdot\mathbf{v} - \rho_{\rm par}\nabla\cdot\mathbf{v} - \frac{d\rho_{\rm sat}}{dT}\frac{DT}{Dt}$$

$$\frac{D\mathbf{v}}{Dt} = -\frac{1}{\rho_{\rm gas}+\rho_{\rm par}}\nabla P$$

$$\rho_{\rm tot}C\frac{DT}{Dt} = -P\nabla\cdot\mathbf{v} + L_{\rm vap}\left(-\rho_{\rm gas}\nabla\cdot\mathbf{v} - \frac{d\rho_{\rm sat}}{dT}\frac{DT}{Dt}\right) - 4\sigma T^4\rho_{\rm par}\kappa$$

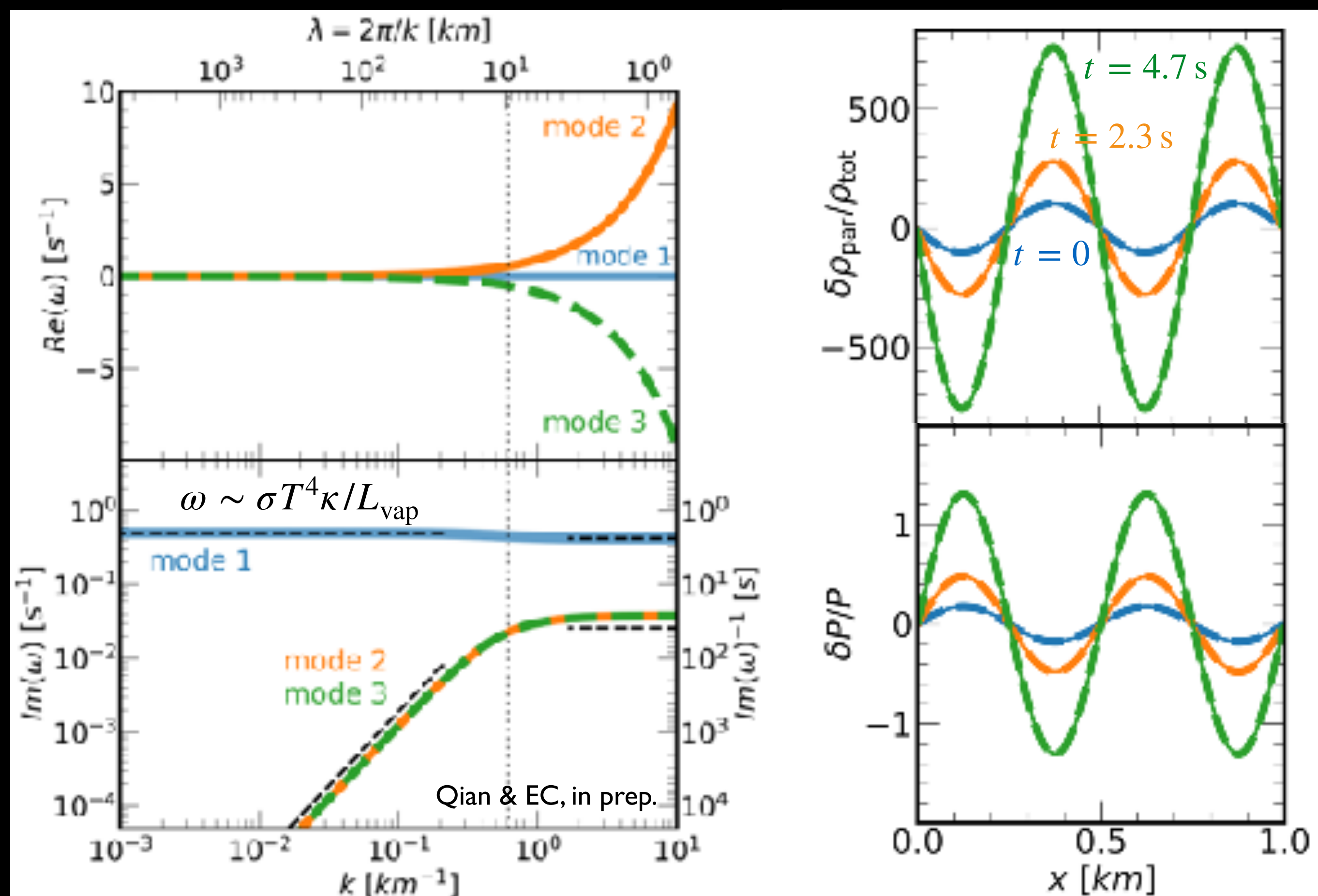

PLANETESIMAL FORMATION BY CAVITATION

Non-linear bubble evolution

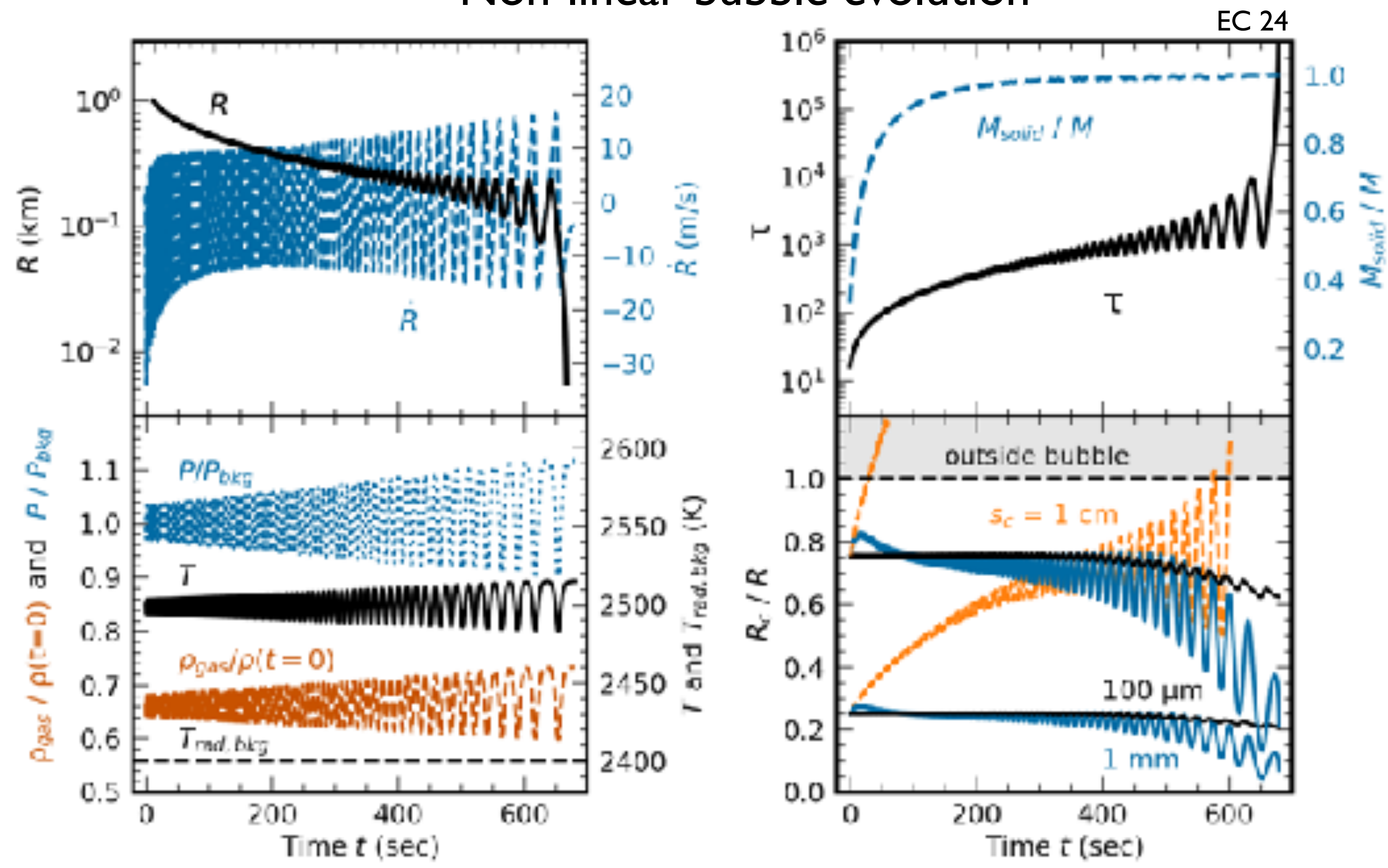

KIC 1255b (Kepler-1520b)

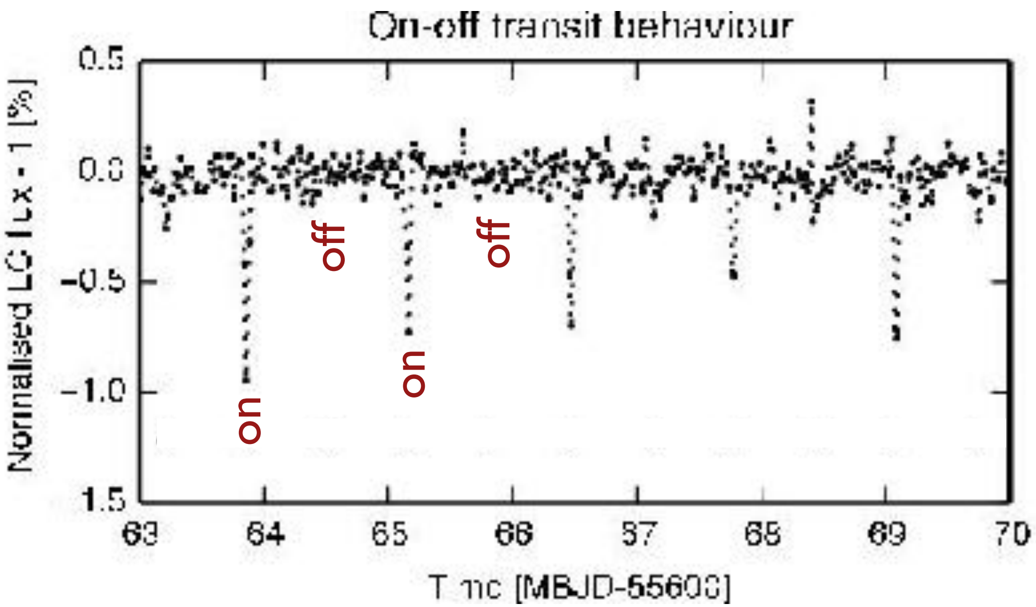

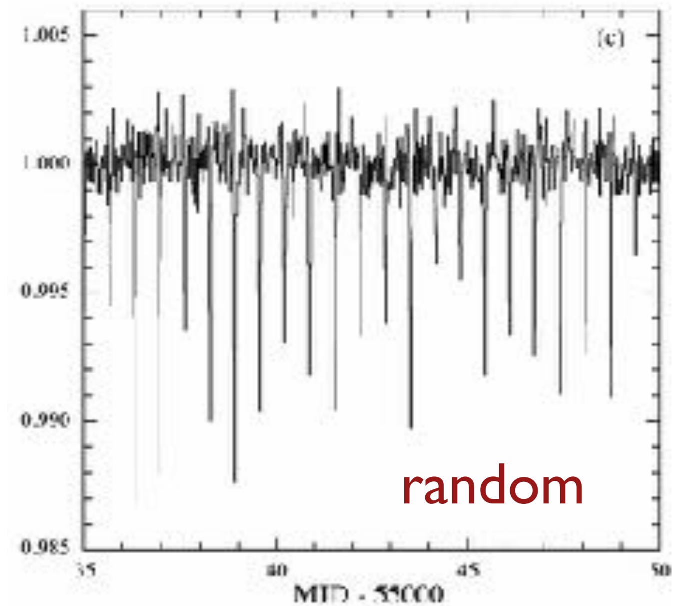

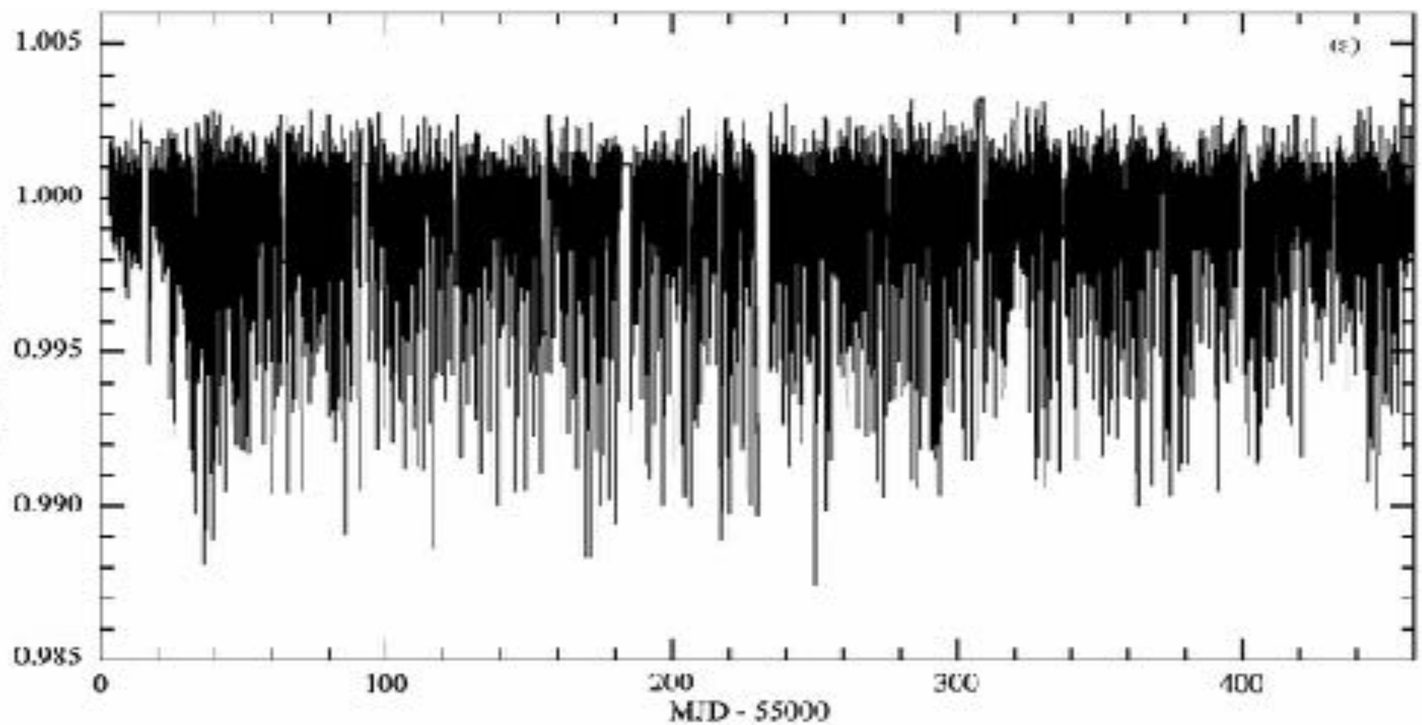

Orbital period
15.685 hr

Effective temperature
2150 K

Random transit depths
< 0.2% to 1.3%

Rappaport, Levine, EC+ 12
van Werkhoven+14

An Ultra-Hot Disintegrating World

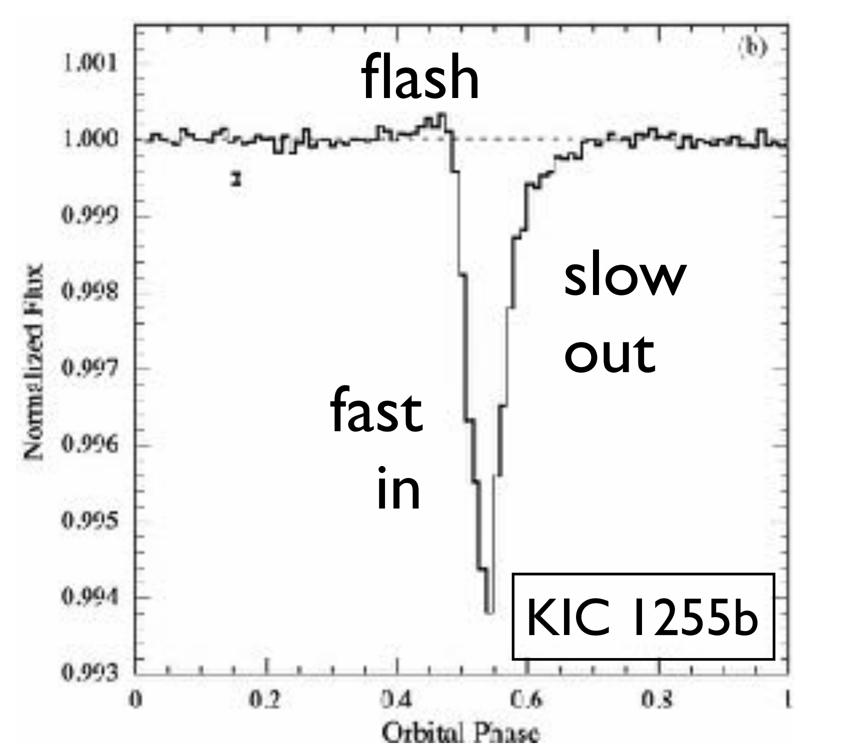

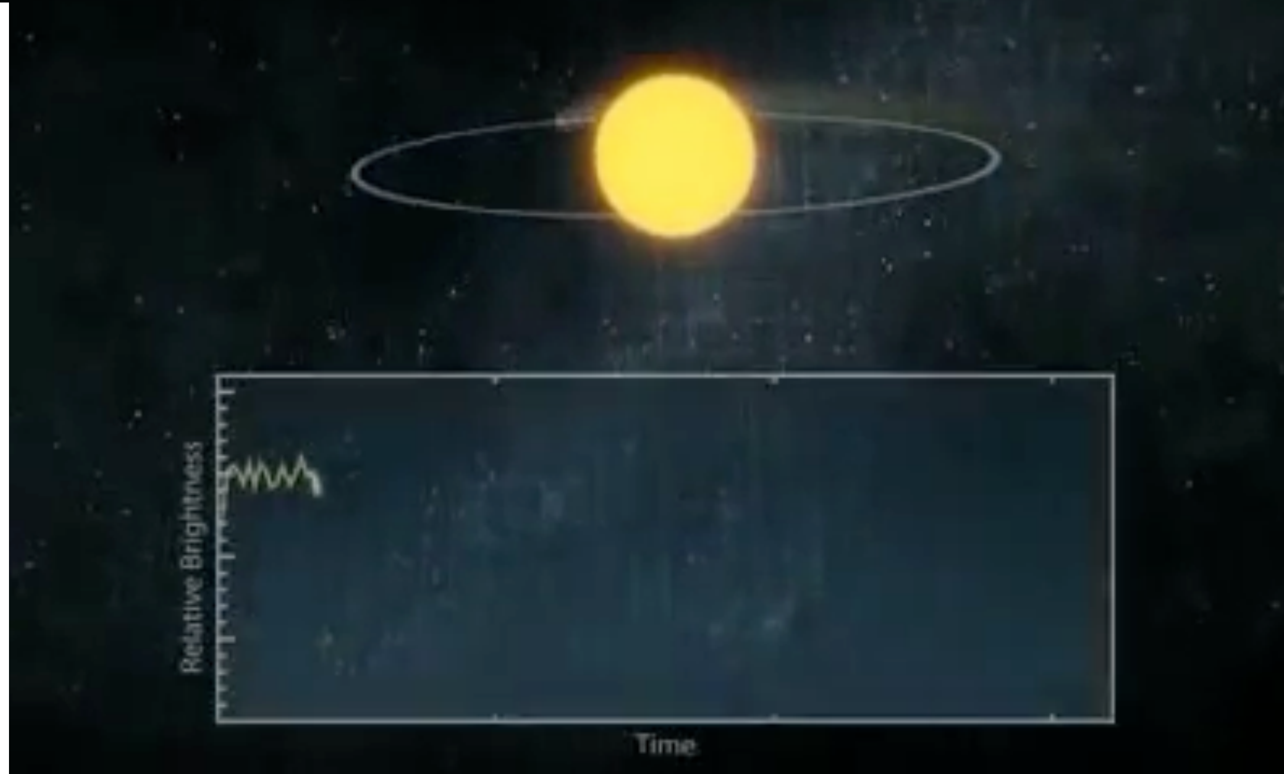

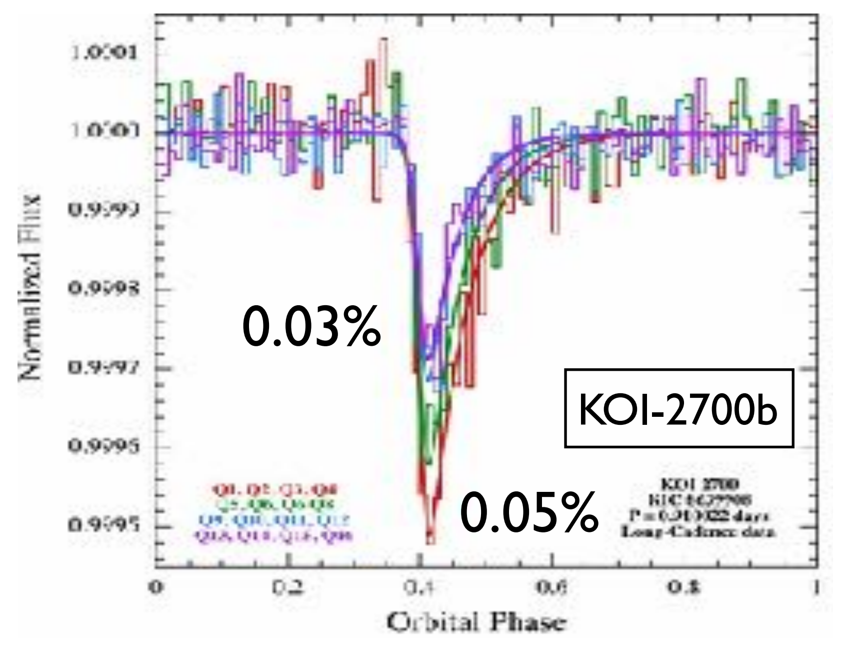

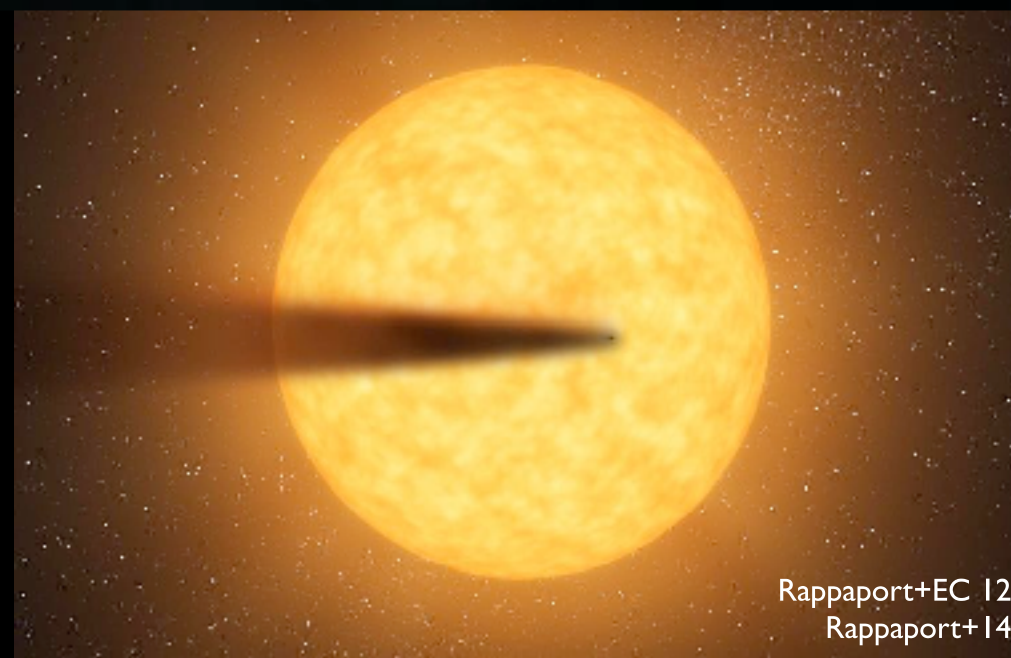

An Ultra-Hot Disintegrating World

$T_{\rm eff} \sim 2100\,{\rm K}$

$\Rightarrow c_s \sim 0.7\,{\rm km/s}$

$\Rightarrow v_{\rm esc} \lesssim$ a few km/s

$\Rightarrow M \lesssim 0.01 M_\oplus$

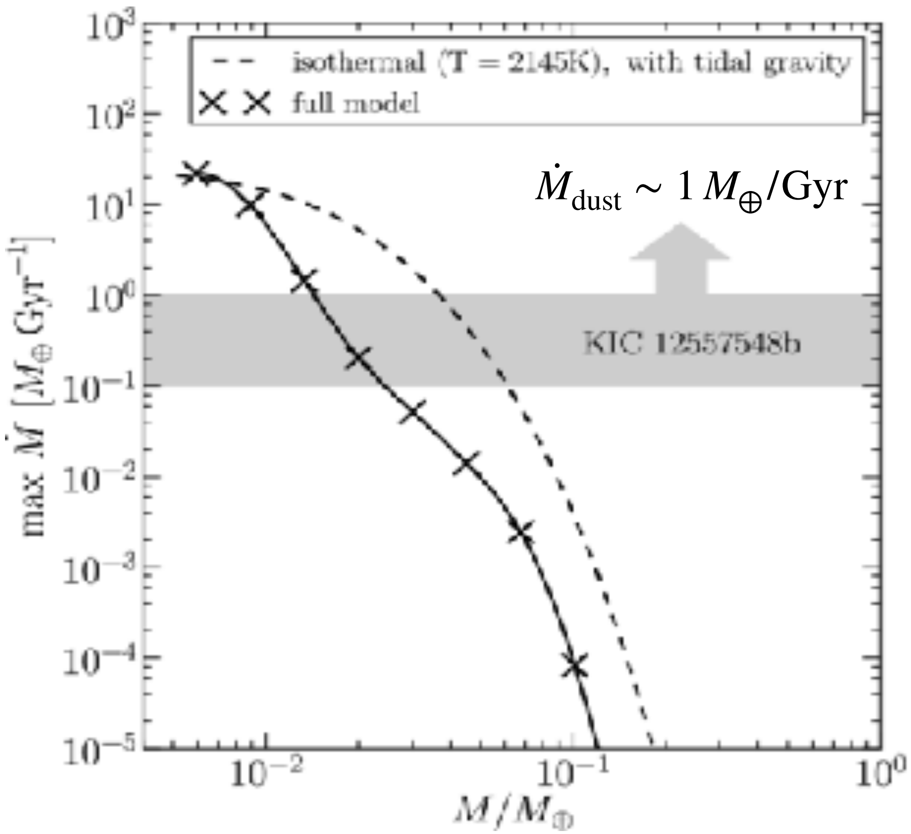

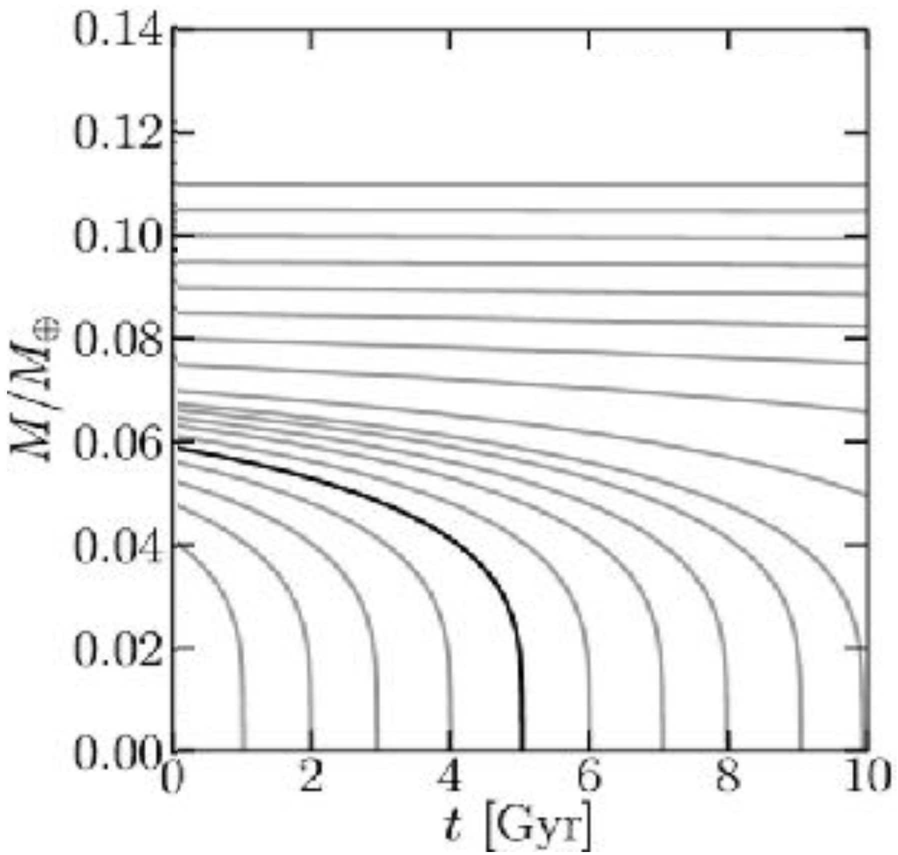

$M \sim 0.01\,M_\oplus \sim 1\,{\rm Moon} \sim 0.2\,{\rm Mercury}$

Perez-Becker & EC 13

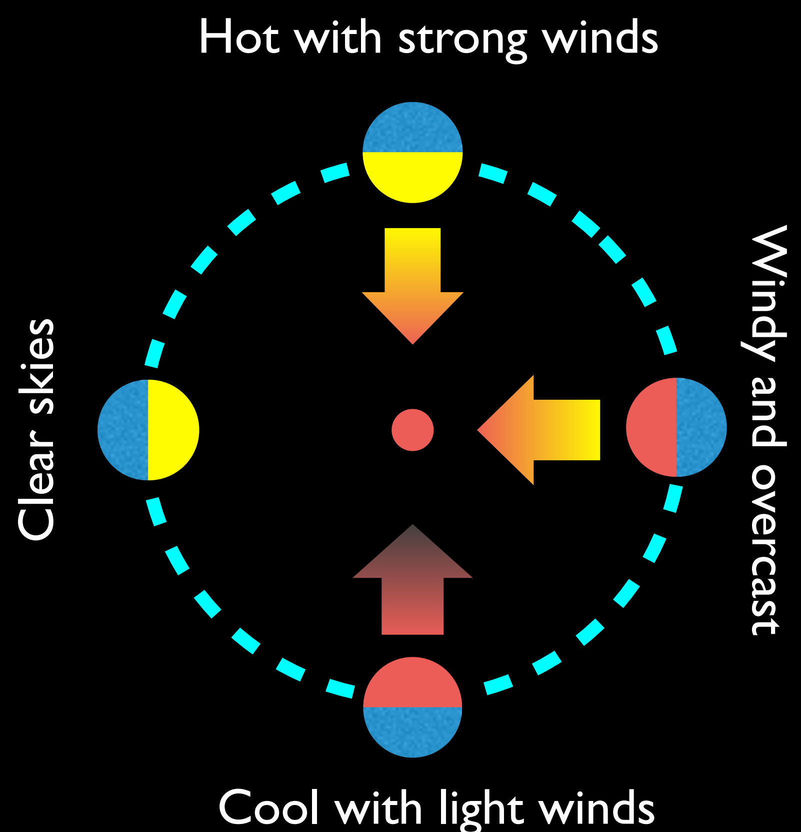

Limit cycle

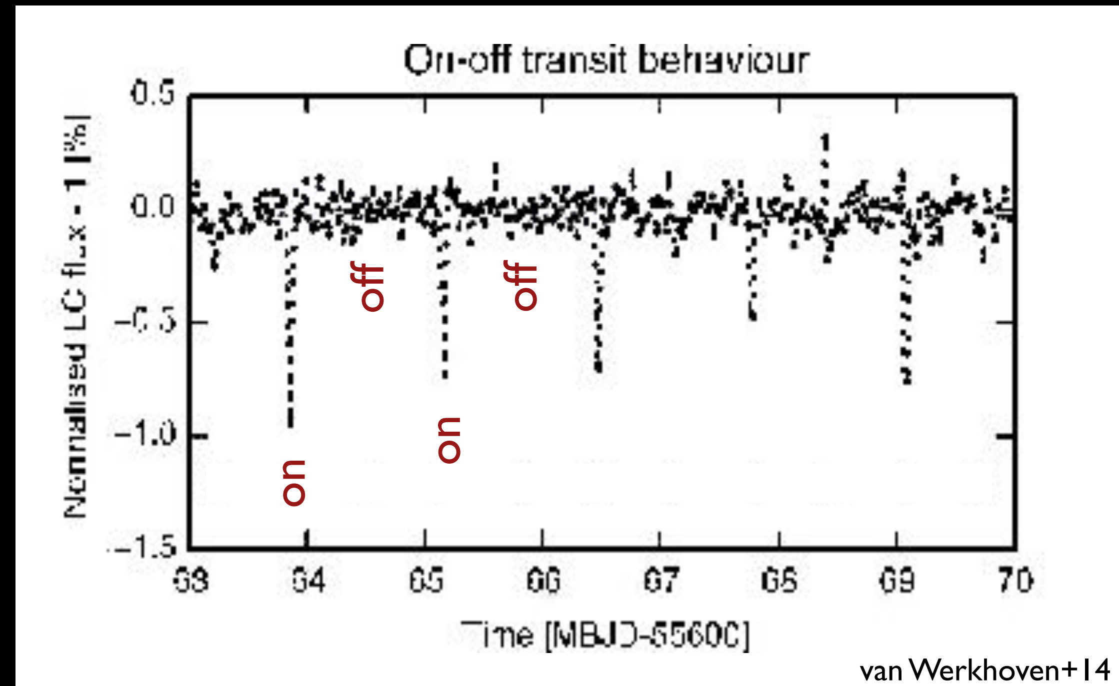

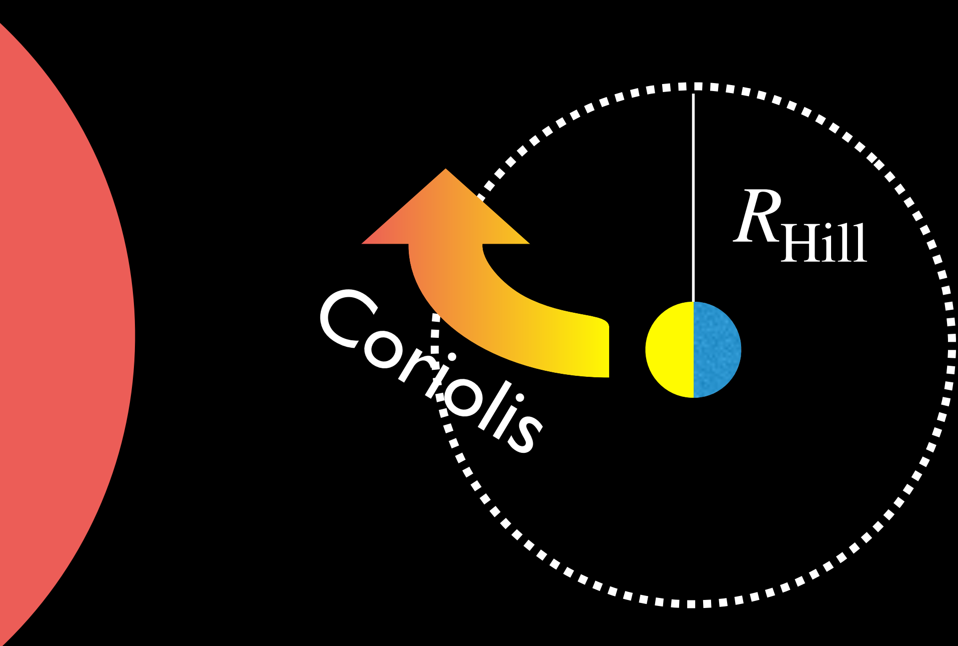

Dynamical time (atmospheric refresh time)

$$\frac{R_{\rm Hill}}{\sqrt{GM_{\rm p}/R_{\rm Hill}}} \sim P_{\rm orb}$$

Perez-Becker & EC 13

Mapping the wind from time i to $i+1$

(1) Mass loss by evaporation (Clausius-Clapeyron)

$$\dot{M}(i) = c_1 \exp\left[-c_2/T(i)\right]$$

(2) Ground temperature and wind optical depth (Eddington two-stream)

$$T(i) = c_3 \left[\left(1 + 1/\gamma\right) + \left(1 - 1/\gamma\right) \exp(-\gamma\tau(i))\right]^{1/4}$$

$$\gamma \equiv \kappa_{\rm V}/\kappa_{\rm IR}$$

(3) Hysteresis

$$\tau(i+1) = c_4 \dot{M}(i)$$

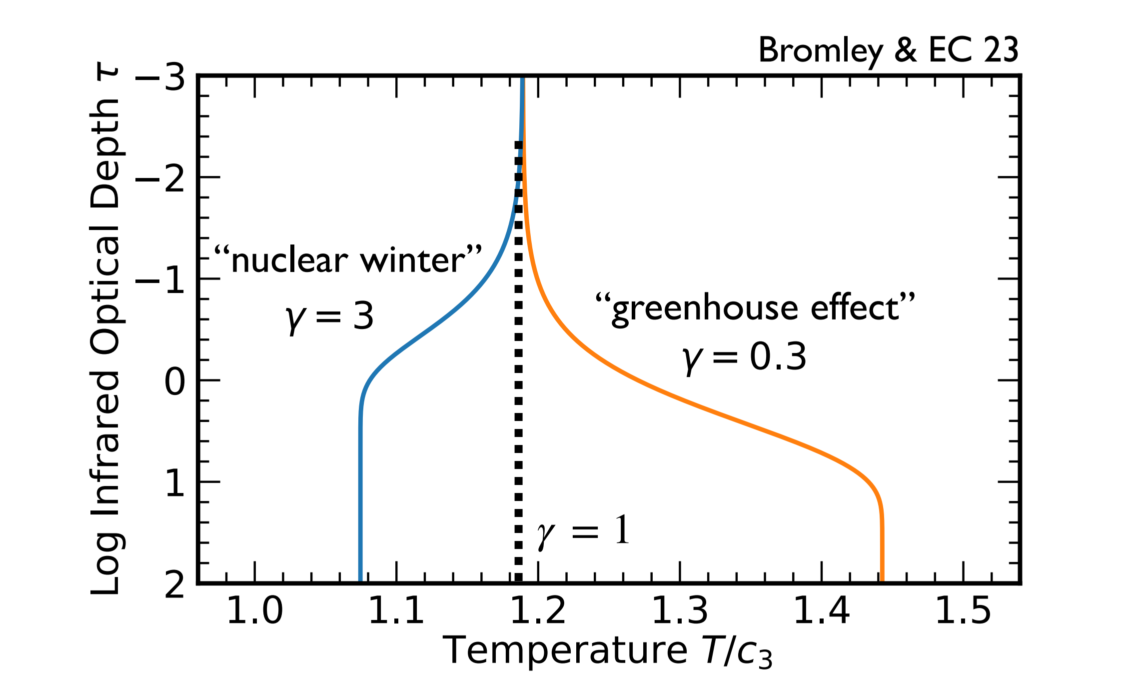

Wind map $\tau(i) \Rightarrow \tau(i+1)$

$$\tau(i+1) = p_1 \exp(2^{-1/4} p_2)\ \exp\{-p_2[(1+1/\gamma) + (1-1/\gamma)\exp(-\gamma\tau(i)]^{-1/4}\}$$

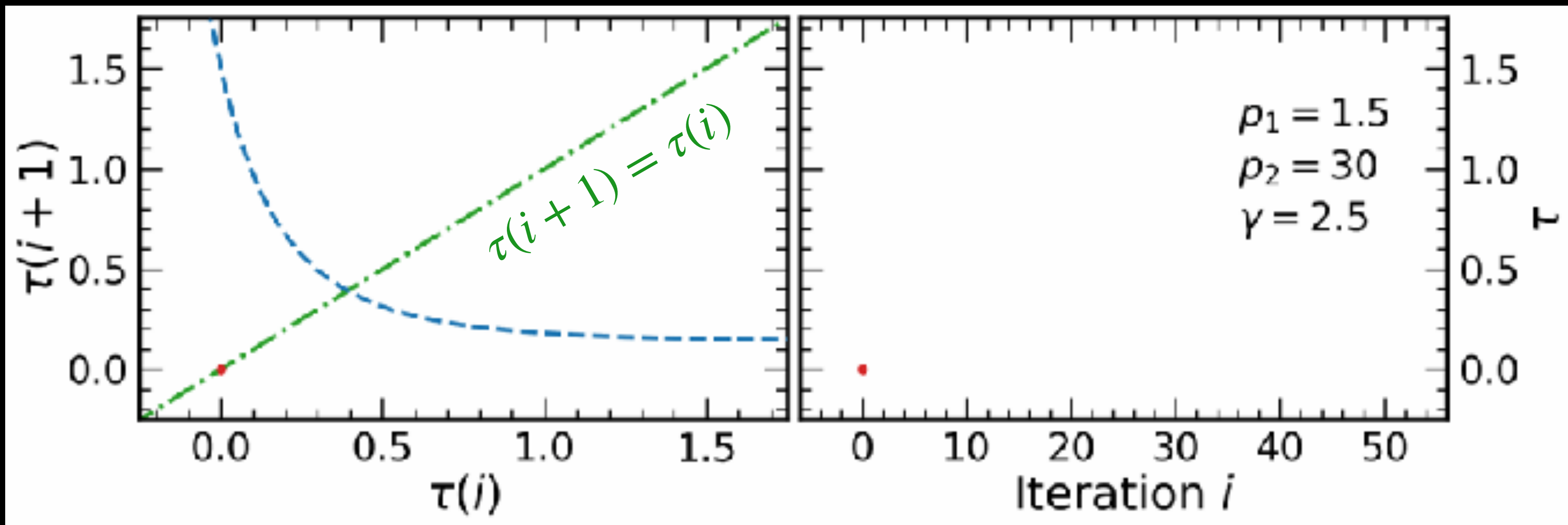

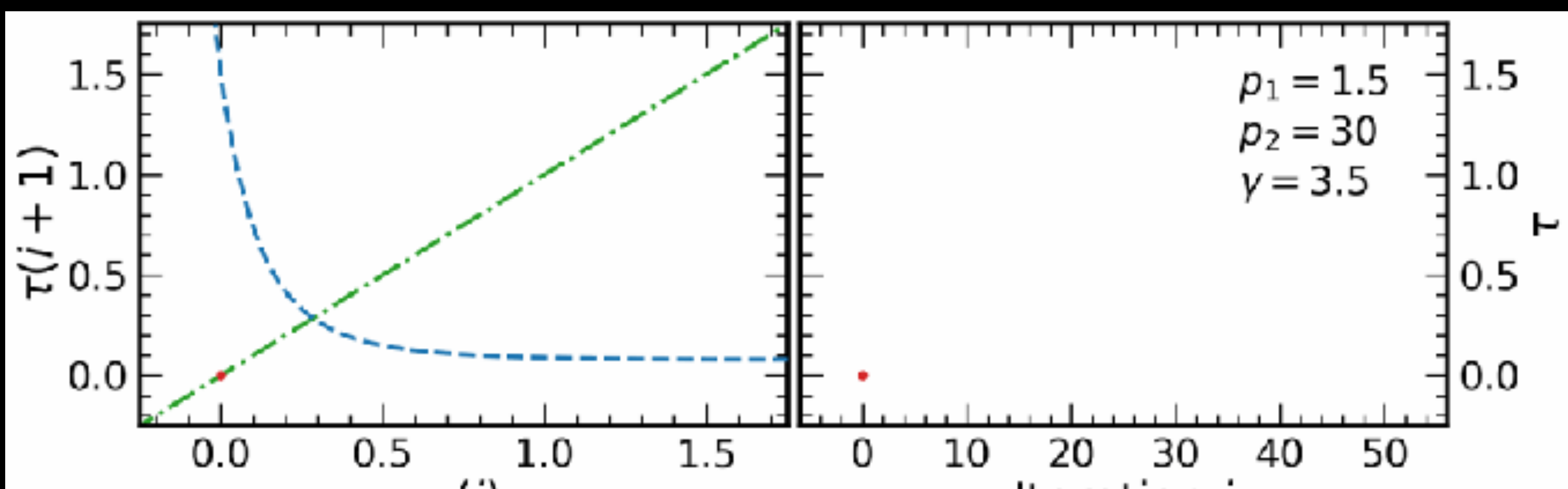

Bromley & EC 23

Dust condensation in strong radiation field

$$T_{\rm star}^4\,\kappa_{\rm V} \propto T_{\rm dust}^4\,\kappa_{\rm IR}$$

Need low $T_{\rm dust}$ to condense

Dust composition will vary with radiation field

iron-poor silicate

$$\gamma = \frac{\kappa_{\rm V}}{\kappa_{\rm IR}} < 1$$

$$\tau \ll 1$$

iron-rich silicate

$$\gamma = \frac{\kappa_{\rm V}}{\kappa_{\rm IR}} > 1$$

$$\tau \gg 1$$

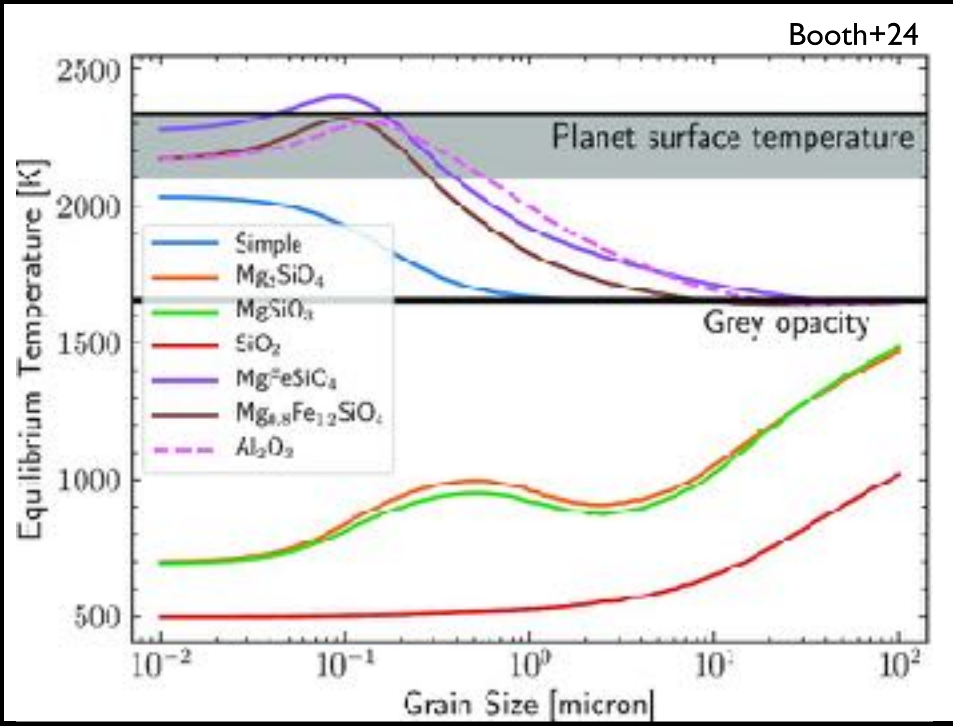

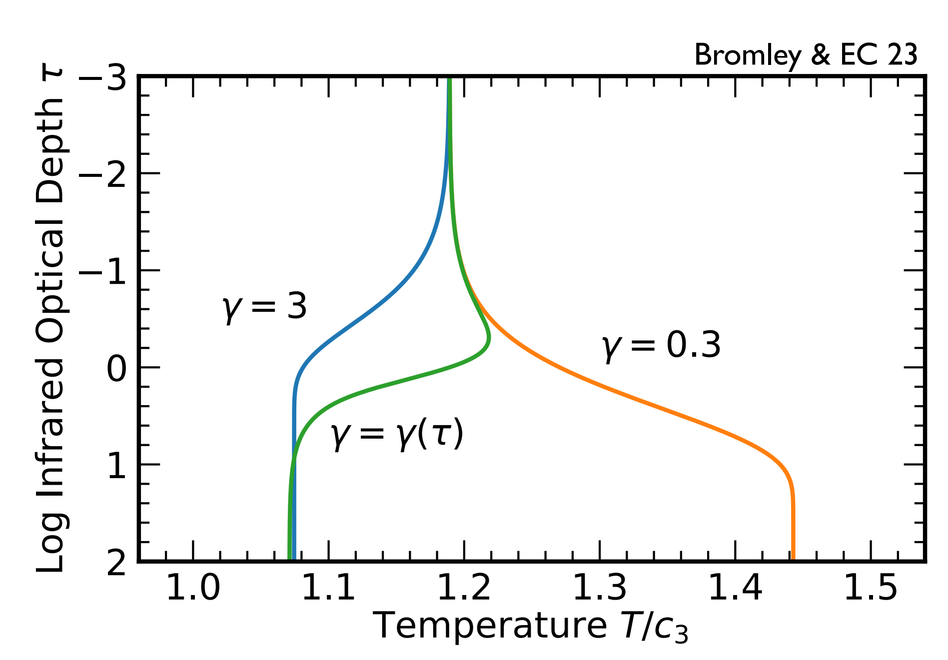

Wind map with $\gamma(\tau)$

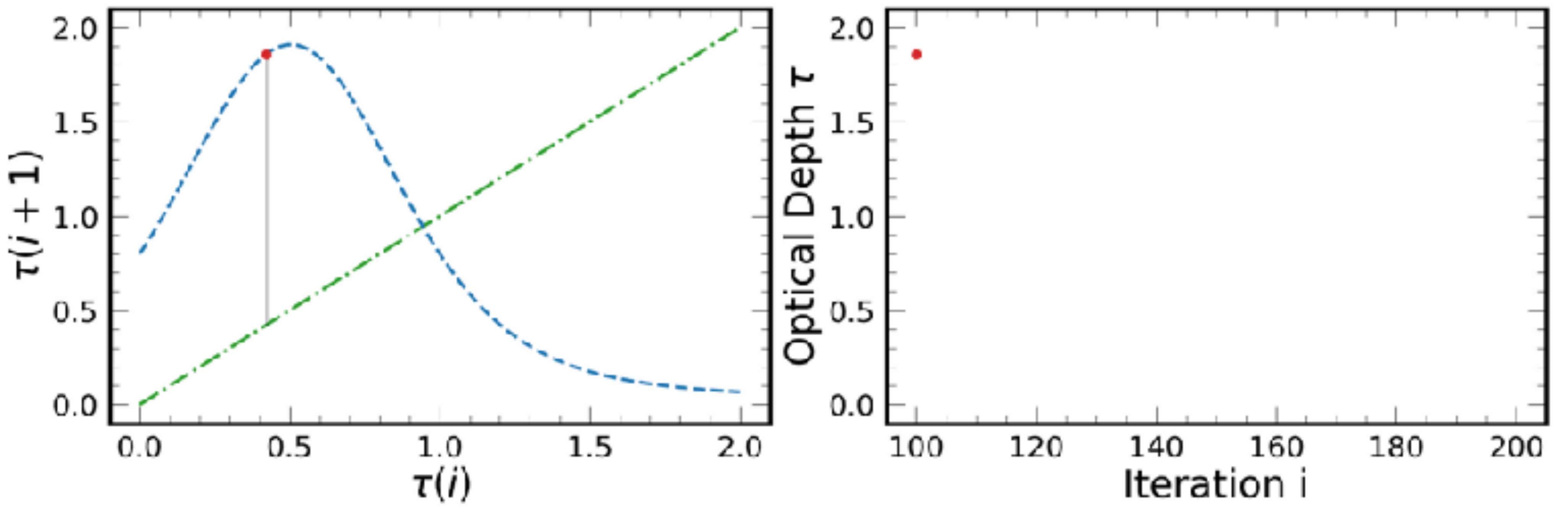

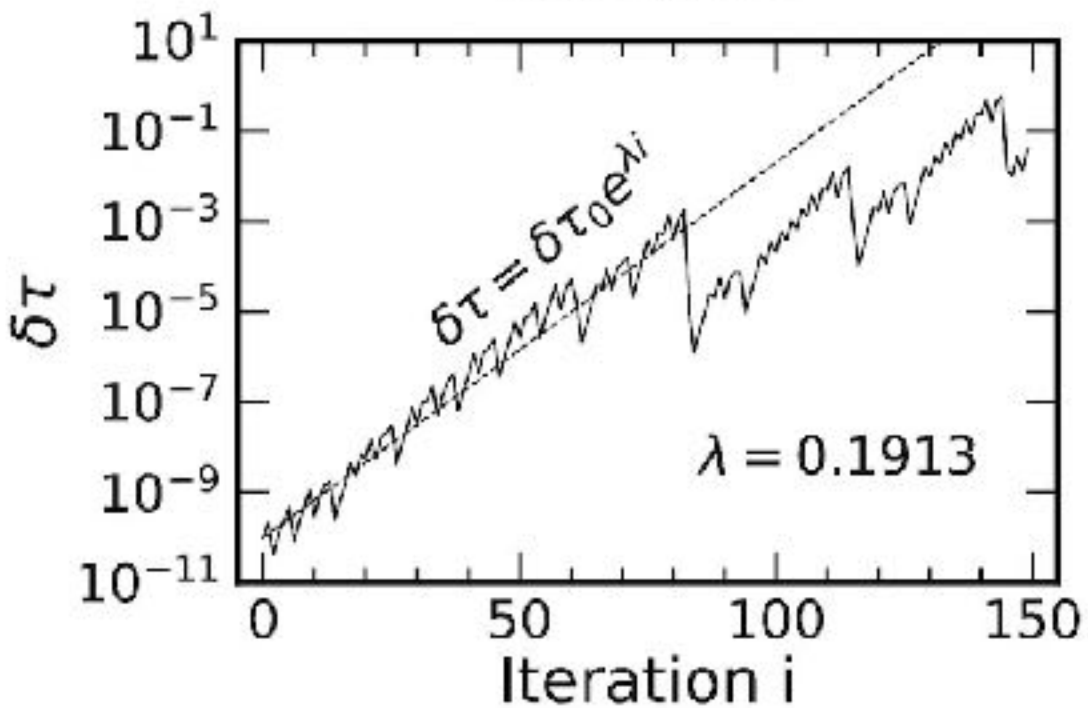

Chaotic divergence of trajectories

Lyapunov time

$\lambda^{-1} \sim 5\,\text{orbits}$

Chaotic disintegration

$$\tau(i+1) = p_1 \exp(2^{-1/4} p_2)\ \exp\{-p_2[(1+1/\gamma(i)) + (1-1/\gamma(i))\exp(-\gamma(i)\tau(i)]^{-1/4}\}$$